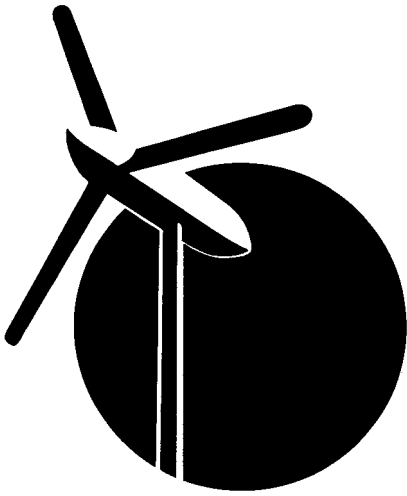


SERI/STR-211-2086
DE84000030

November 1983



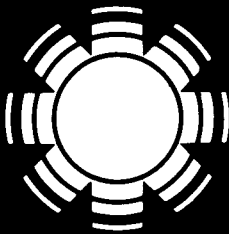
Television Interference Measurements Near the MOD-2 WT Array at Goodnoe Hills, Washington

A Subcontract Report

D. L. Sengupta
T. B. A. Senior
J. E. Ferris

Radiation Laboratory
University of Michigan
Ann Arbor, Mich.

Prepared under Subcontract No. DE-AC02-76ET20234



SERI

Solar Energy Research Institute

A Division of Midwest Research Institute

1617 Cole Boulevard
Golden, Colorado 80401

Operated for the

U.S. Department of Energy

under Contract No. DE-AC02-83CH10093

Printed in the United States of America
Available from:
National Technical Information Service
U.S. Department of Commerce
5285 Port Royal Road
Springfield, VA 22161
Price:
Microfiche A01
Printed Copy A04

NOTICE

This report was prepared as an account of work sponsored by the United States Government. Neither the United States nor the United States Department of Energy, nor any of their employees, nor any of their contractors, subcontractors, or their employees, makes any warranty, express or implied, or assumes any legal liability or responsibility for the accuracy, completeness or usefulness of any information, apparatus, product or process disclosed, or represents that its use would not infringe privately owned rights.

SERI/STR-211-2086
UC Category: 60
DE84000030

**Television Interference
Measurements Near the
MOD-2 WT Array at
Goodnoe Hills, Washington**
A Subcontract Report

D. L. Sengupta
T. B. A. Senior
J. E. Ferris

Radiation Laboratory
University of Michigan
Ann Arbor, Mich

November 1983

Prepared under Subcontract No. DE-AC02-76ET20234

SERI Technical Monitor: Neil D. Kelley

Solar Energy Research Institute

A Division of Midwest Research Institute

1617 Cole Boulevard
Golden, Colorado 80401

Prepared for the

U.S. Department of Energy

Contract No. DE-AC02-83CH10093


PREFACE

The authors gratefully acknowledge the assistance of various individuals in the completion of the measurement program. They are particularly grateful to K. Cavcey and L. Lee of the Bonneville Power Administration (BPA), and R. Schwemmer, J. Peetz, and G. Soranaka of the Boeing Engineering & Construction Company for providing us with the necessary help at the test sites. Successful completion of the program would not have been possible without the coordinating efforts of N. Kelley of SERI and M. Reynolds and P. Renner of BPA. The authors also wish to thank Wanita Rasey for her help in preparing the draft.



Neil D. Kelley, Technical Monitor

Approved for
SOLAR ENERGY RESEARCH INSTITUTE



Donald Ritchie, Manager
Solar Electric Conversion Research
Division

SUMMARY

Electromagnetic interference to television reception caused by the MOD-2 wind turbine (WT) array at Goodnoe Hills, Wash., has been studied by carrying out detailed measurements at a number of test locations or sites in the vicinity of the WT array. The commercial television (TV) signals available in the area were used as the radio frequency (rf) sources during the measurements. Tests were performed at the top of the WT No. 2 tower and at the bases of the three WT towers, and at three other sites chosen to represent the region around the WT array. For some TV channels, all of the sites were in the backward interference region of the WTs, but for other channels, some of the sites were also in the forward interference region.

At each location, some or all of the following types of measurement were performed on all of the available TV channels: (i) Received field strength. With the WTs stationary, the strength of the received signal was measured by rotating the main beam of the receiving antenna until the output was maximum. This provided information about the expected quality of TV reception in the area, and also the field strengths of various TV channels at the WT No. 2 relative to those at a test site, which play an important role in the television interference (TVI) effects produced by the WTs. (ii) Static or blade scattering. With the blades of WT No. 2 locked in a desired (usually horizontal) position and their pitch set for maximum power, the WT was yawed in azimuth through 360° . Measuring the TV signals received with the antenna pointed at the WT helped to determine the maximum blade-scattered signals. From these results, the equivalent scattering area (A_e) and length (L_1) of the blades were determined. These measurements were important because the interference caused by the WT depends critically on these parameters. (iii) In some cases, as the antenna was rotated the output of the receiver was recorded as a function of time, with and without the WT blades rotating. These measurements served to determine (a) the horizontal plane pattern of the antenna in an actual test environment, (b) the effect of the WTs on the received signal, and (c) the amount of signal modulation caused by the operating turbines. (iv) Dynamic or television interference (TVI). These tests were performed with the WT(s) operating and by recording the received signal versus time with the antenna directed at the desired transmitter or at the WT array, while the received picture was observed on the TV screen for any video distortion. Dynamic measurements were performed at first with one WT operating, then two, and finally all three WTs operating together. The equipment setup and the measurement procedures were similar to those employed in our previous studies. Directional receiving antennas were used at all test sites.

The ambient field strength measurements indicated that in the region surrounding the WT array, all of the TV signals are extremely weak, and the quality of TV reception in the area is generally very poor to unacceptable. The field strengths on top of the WTs were generally of the same order as those at the remote test sites.

The equivalent scattering area of the MOD-2 blade, determined from static tests using two different channels at one site and one channel at a second site, was very close to the 184 m^2 predicted on the basis of laboratory measurements of scale-model MOD-2 blades.

The dynamic measurements indicated that (a) varying amounts of TVI were produced at all sites and on some or all of the available TV channels; (b) with the directional antenna in use, most of the backward region interference produced video distortion that was judged to be acceptable; (c) at one test location about 1-1/2 miles from the WT array site, forward region interference was observed on Channel 12; (d) when the blades of the WTs rotate in synchronism, they tend to increase the amplitude of the interference pulses, thereby producing more TVI effects; and (e) when the blades do not rotate in synchronism, each WT produces interference effects individually.

TABLE OF CONTENTS

	<u>Page</u>
1.0 Introduction.....	1
2.0 Background Information.....	3
2.1 Physical Environment.....	3
2.2 The MOD-2 WT.....	3
2.3 Test Sites.....	6
2.4 The Interference Phenomenon.....	9
2.5 Available TV Signals.....	13
3.0 Test Equipment and Procedures.....	15
3.1 Equipment.....	15
3.2 The Receiving Antennas.....	17
3.3 Types of Measurement.....	17
4.0 Measured Ambient Signal Strengths.....	19
4.1 Received Signal Strength and Quality of Reception.....	19
4.2 Signal Strengths at the WT Array Site.....	20
4.3 Signal Strengths at Sites A, B, and C.....	21
4.4 Conclusions.....	22
5.0 Blade Scattering (Static Tests).....	23
5.1 Comments on the Blade Scattering Parameters.....	23
5.2 Procedure.....	24
5.3 Results.....	24
5.4 Theoretical Expressions.....	28
5.5 Data Analysis.....	30
5.6 Discussion.....	33
6.0 Television Interference Measurements (Dynamic Tests).....	35
6.1 Site A.....	35
6.2 Site B.....	39
6.3 Site C.....	39
6.4 Discussion.....	42
7.0 Conclusions.....	45
8.0 References.....	47
Appendix: Theoretical Considerations.....	49
A.1 Scattering by a Rectangular Metal Plate.....	49
A.2 Received Field During Static Measurements.....	53

LIST OF FIGURES

	<u>Page</u>
2-1 A General Roadmap of the Region Surrounding the WT Array Site.....	4
2-2 A Sketch of the Immediate Area Indicating the Approximate Locations of the Three MOD-2 Machines.....	5
2-3 Detailed Sketch of the WT Cluster Site.....	6
2-4 Topographical Map of the Terrain Surrounding the WT Array.....	7
2-5 Engineering Sketch of a MOD-2 WT.....	9
2-6 Geometry of the WT Blade Scattering.....	11
2-7 Theoretical Interference Zone for TV Channel 11 with Transmitter 50 km Away.....	12
2-8 Location of the Available TV Signal Transmitters with Respect to the WT Array and the Test Sites.....	14
3-1 Schematic Block Diagram of the Measurement System.....	16
5-1 E_a (dB μ V) vs. WT No. 2 Yaw Angle on Channel 6, Obtained at Site A.....	25
5-2 E_a (dB μ V) vs. WT No. 2 Yaw Angle on Channel 8, Obtained at Site C.....	26
5-3 E_a (dB μ V) vs. WT No. 2 Yaw Angle on Channel 6, Obtained at Site C.....	27
5-4 Horizontal Plane Geometry of the Blade, the Receiver, the Incident and Scattered Field Directions.....	29
5-5 Elevation Plane Geometry of the Blade, the Receiver, the Incident and Scattered Field Directions.....	29
6-1 E_a (dB μ V) vs. Time on Channel 19, Obtained at Site A.....	36
6-2 E_a (dB μ V) vs. Time on Channel 19, Obtained at Site A.....	37
6-3 E_a (dB μ V) vs. Time on Channel 19, Obtained at Site A.....	38
6-4 E_a (dB μ V) vs. Time on Channel 42, Obtained at Site A.....	40

LIST OF FIGURES (Concluded)

	<u>Page</u>
6-5 E_a (dB μ V) vs. Time on Channel 12, Obtained at Site B.....	41
6-6 E_a (dB μ V) vs. Time on Channel 6, Obtained at Site C.....	43
6-7 E_a (dB μ V) vs. Time on Channel 6, Obtained at Site C.....	44
A-1 Rectangular Metal Plate with the Incident Field Direction and the Receiver Location Shown.....	50

LIST OF TABLES

	<u>Page</u>
2-1 MOD-2 2500-kW Wind Turbine Design Specifications.....	8
2-2 Site Information.....	10
3-1 Gain Characteristics of the Winegard Antenna Relative to the Biconical Antenna.....	18
4-1 Received Field Strengths at the Bases of WT Nos. 1 and 3 with the Receiving Antenna Located 38.5 ft Above the Ground.....	20
4-2 Received Field Strengths at the Base and on Top of WT No. 2.....	21
4-3 Field Strengths at the Remote Test Sites Received with Biconical (VHF) and Logconical (UHF) Antennas Located 38.5 ft Above the Ground.....	21
5-1 Equivalent Scattering Parameters for the MOD-2 Blade Obtained from Full-Scale Measurements.....	32



SECTION 1.0

INTRODUCTION

A cluster of three MOD-2 wind turbines (WTs) has been installed and is in operation at a site near Goodnoe Hills, Wash. [1]. From May 3 to May 15, 1982, University of Michigan Radiation Laboratory conducted a series of television interference (TVI) measurements near the WT array site. Although our laboratory previously conducted similar measurements at a number of other sites containing single horizontal-axis WTs [2,3], and developed theoretical methods [4] to estimate the TVI effects produced by such machines, the present measurements were necessary because (a) the TVI effects are site-specific and, more importantly, the interference effects of WTs operating in a cluster were not known; and (b) because the design of the MOD-2 blade is different from that of the MOD-1 type of blades studied earlier, the equivalent scattering parameters for the former obtained theoretically from scale-model considerations based on the MOD-1 blade [4,5] required confirmation by actual measurements.

The goals of the present measurements were to (i) obtain an estimate of the equivalent scattering area (A_e) and length (L_e) of the full-scale MOD-2 blade, and (ii) estimate the TVI effects produced by such machines operating in a cluster. The measurements were conducted by receiving commercially available TV signals at selected locations in the vicinity of the WT array site. In the following sections we describe these on-site measurements and discuss the results obtained and their implications.



SECTION 2.0

BACKGROUND INFORMATION

2.1 PHYSICAL ENVIRONMENT

The MOD-2 WT array is located about 106 miles due east of Portland, Ore., on the northern shore of the Columbia River; the turbine array site is identified in a section of the general road map of the region shown in Figure 2-1. The turbines are actually located in the State of Washington at a place approximately 13 miles east of Goldendale, Wash. Figure 2-2 shows a sketch of the immediate area indicating the locations of the three MOD-2 machines (1, 2, and 3, respectively) west of Goodnoe Hills, Wash.; a more detailed sketch of the WT cluster site is shown in Figure 2-3. These three machines, presently operating together, compose the nation's first cluster of large-scale, multimegawatt wind turbines [1].

The terrain around the turbines is generally hilly. A portion of the topographical map (prepared by the U.S. Geological Survey) of the terrain within a five-mile radius of the WT array site is shown in Figure 2-4 where we have again identified the three turbines as 1, 2, and 3, respectively. Figures 2-3 and 2-4 indicate that all three turbines are located at higher elevations than the local terrain.

2.2 THE MOD-2 WT

The MOD-2 WT, shown in the sketch in Figure 2-5, is an upwind horizontal-axis machine designed and built by the Boeing Engineering and Construction Company. Its mechanical system consists of two propeller-type rotor blades; the rotor is attached to a low-speed shaft that transmits the torque from the rotor to a gear box, which converts the relatively slow rotor speed into the high-speed rotation necessary to drive the generator. The resulting electrical power is channeled into a utility power grid. Thus, the MOD-2 system comprises a rotor; a nacelle, which houses the major subsystems such as the drive train, the generator, the yaw bearing, the yaw drive, and associated subsystems for pitch/yaw control; safety systems; the tower; and the foundation [1].

The rotor and nacelle are mounted on top of a cylindrical steel shell tower with a height of 200 ft above the ground. The generator is driven by horizontal-axis steel blades which have a total length of 300 ft tip to tip. The 45-ft blade tip sections can be rotated to provide a variable pitch capability. The blade can also teeter so that its rotational axis is tilted up to 6° in the vertical plane from the rotational axis of the generator. Actually, the machine teeters automatically according to wind speed and direction, and the amount of teetering cannot be controlled. However, the tip pitch angle and the yaw position of the nacelle can be metered and controlled. The machines are controlled in a manner similar to that of the MOD-OA or the MOD-1 WT; i.e., they are computer-controlled. The computer receives input data regarding the wind speed and direction; this information is then processed by the computer to determine the required yaw and pitch position of the blade for optimum operation.

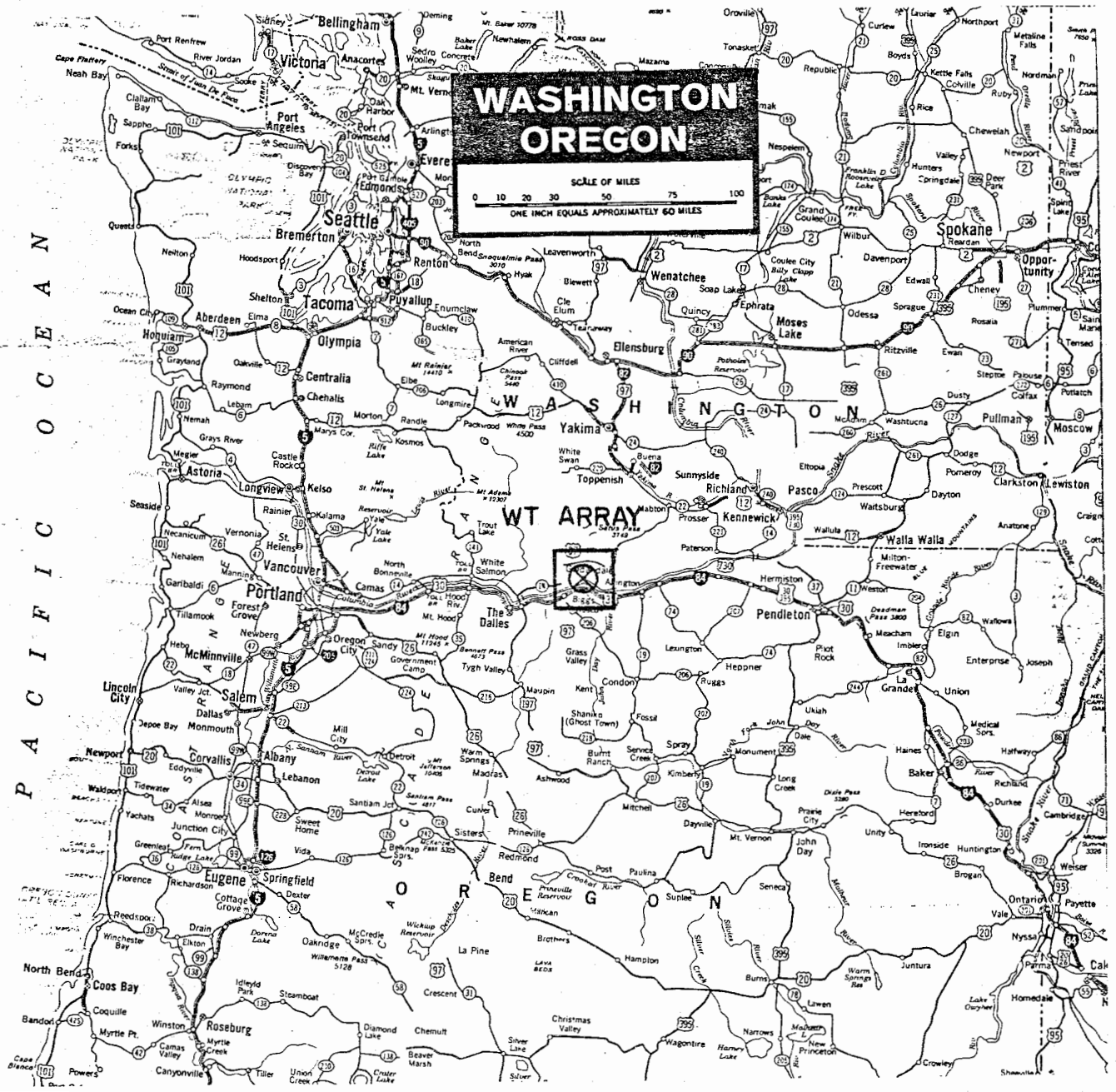


Figure 2-1. A General Roadmap of the Region Surrounding the WT Array Site

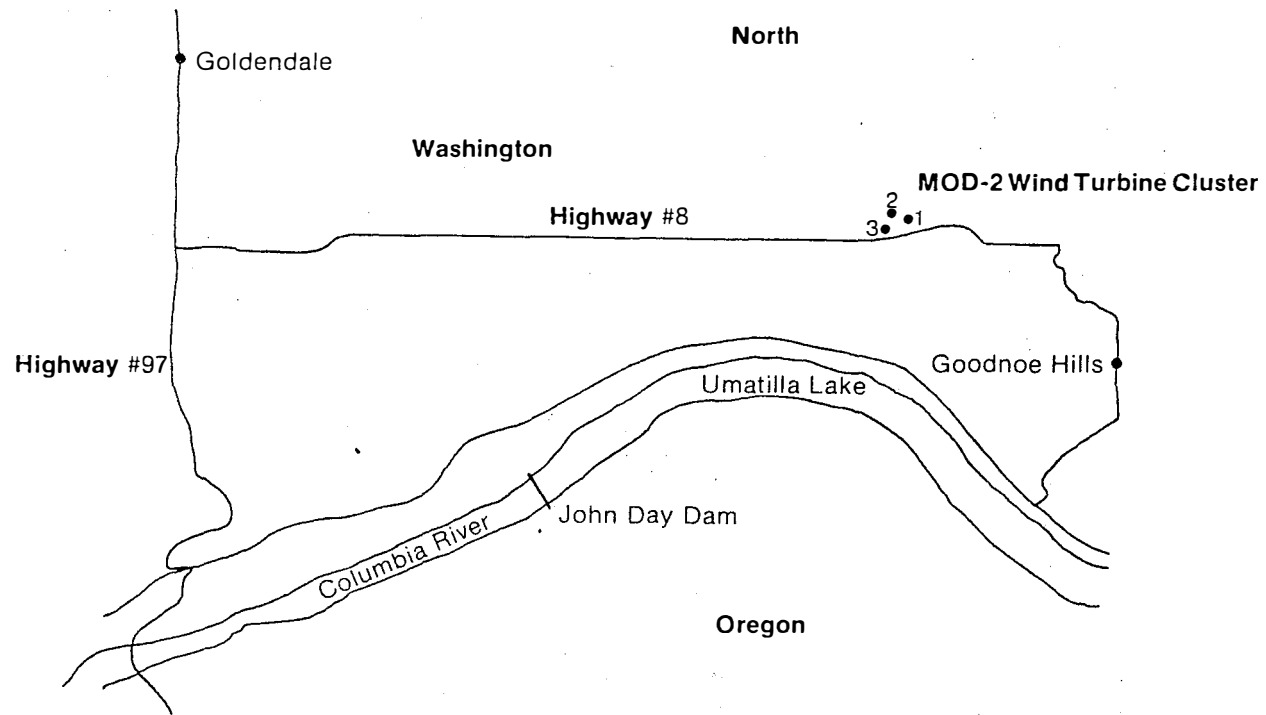


Figure 2-2. A Sketch of the Immediate Area Indicating the Approximate Locations of the Three MOD-2 Machines

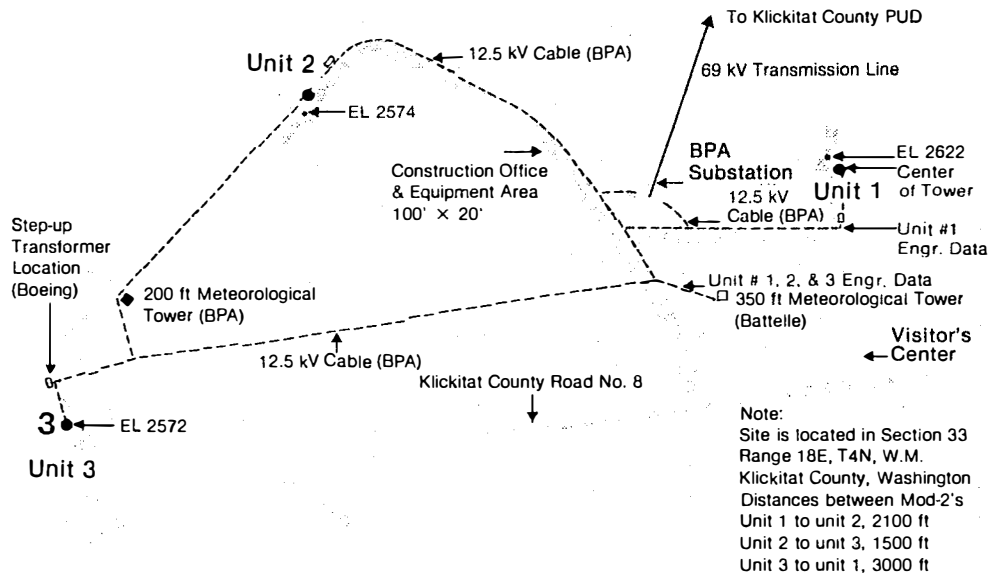


Figure 2-3. Detailed Sketch of the WT Cluster Site

The machines are designed to operate at a constant blade rotation of 17.5 rpm, which does not vary as a function of the wind speed. The most desirable wind-speed regime for the MOD-2 operation is between 27.5 and 45 mph [1]. The MOD-2 cut-in wind speed is 14 mph; when the average wind speed exceeds 45 mph for a short length of time, the WT automatically stops or "cuts out." The power produced by a MOD-2 WT varies from 200 kW at cut-in speed (14 mph) to 2500 kW, achieved when the wind speed reaches 27.5 mph or greater. The relevant specifications of the MOD-2 WT are provided in Table 2-1.

The three MOD-2 WTs that make up the WT array are of identical design. The combined capacity of the three machines produces 7.5 MW of electricity into the transmission lines of the Bonneville Power Administration (BPA), and the system is designed to be available 90% of the time the wind blows [1].

2.3 TEST SITES

Most of the measurements were carried out at three test sites--referred to as A, B, and C in Figure 2-4. These sites were selected to provide TVI data representative of the forward and backward regions of the turbines, which are described in a later section. Relevant information regarding the geometry of the test sites is given in Table 2-2. Sites A and B are located approximately one mile from the center of the WT array, and are west and east, respectively, of the array site along the road which passes immediately to the south of the WTs. Site C is located approximately four miles to the west of the center of the WT array. The elevations of Sites A and C are about 200 and 600 ft, respectively, below that of the center of the WT array; the elevation of Site B is approximately the same as that of the WT array center.

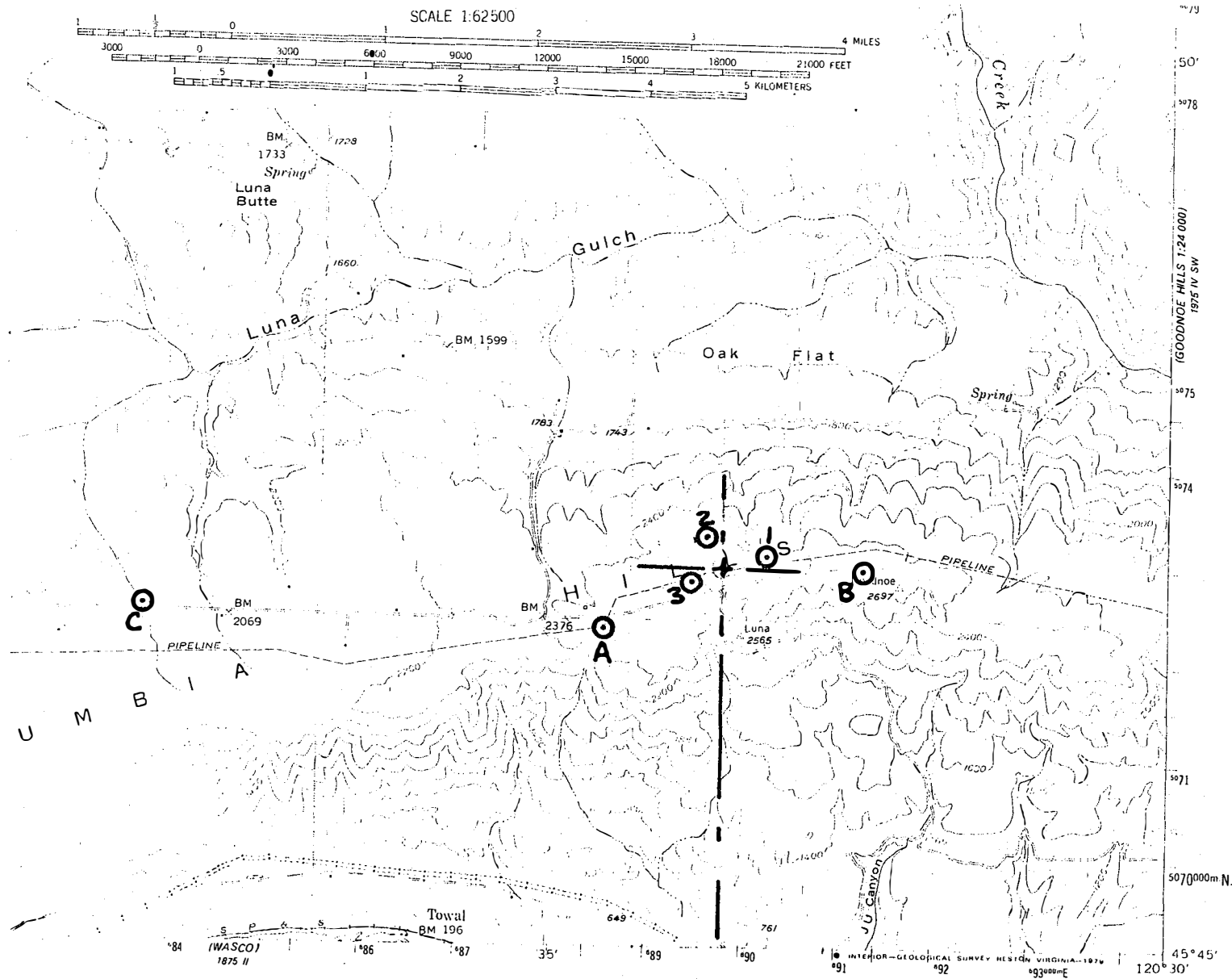


Figure 2-4. Topographical Map of the Terrain Surrounding the WT Array

Table 2-1. MOD-2 2500-kW Wind Turbine Design Specifications

<u>Rotor</u>		<u>Gearbox</u>	
Diameter (ft)	300	Type	Three-stage planetary
Speed (rpm)	17.5	Gear step-up ratio	103
Number of blades	2	Rating (hp)	3700
Direction of rotation	Counterclockwise (looking upwind)	<u>Generator</u>	
Location relative to tower	Upwind	Type	Synchronous ac
Type of hub	Teetered	Rating (kVA)	3125
Cone angle (deg.)	0	Power factor	0.8
Tilt angle (deg.)	2	Voltage	4160 (three phase)
Method of power regulation	Tip pitch control	Speed (rpm)	1800
Material	Steel	Frequency (Hz)	60
Hub length (ft)	6	<u>Control System</u>	
Mid-section length (ft)	75	Supervisory	Microprocessor
Tip length (ft)	45	Pitch actuator	Hydraulic
Airfoil	NACA 230XX	<u>Performance</u>	
Solidity Ratio	0.03	Rated power (kW)	2500
Twist (deg.)	8	Wind speed at 30 ft (at hub) (mph)	
Tip chord (ft)	4.7	Cut-in	9 (14)
Taper ratio	3:1	Rated	20 (27.5)
<u>Yaw Drive</u>		Cut-out	36 (45)
Type	Internal tooth ring gear	Maximum design	120 (125)
Yaw rate (deg./sec)	0.25	<u>Weight (1000 lb)</u>	
Yaw motor	Hydraulic	Rotor	180
<u>Tower</u>		Above tower (includes rotor)	364
Type	Flared shell	Tower	255
Height (ft)	192	Total	619
Hub height (ft)	200	<u>System Life</u>	
Access	Power manlift	All components (yr)	30

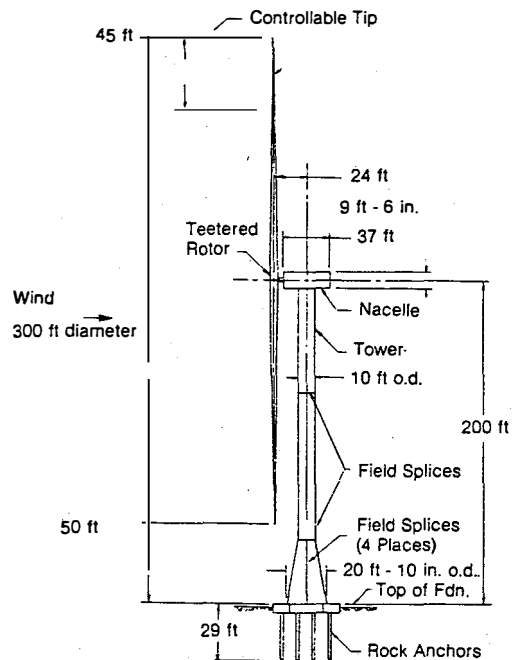


Figure 2-5. Engineering Sketch of a MOD-2 WT

In addition to Sites A, B, and C, a limited amount of TVI measurements were also carried out at other selected locations, which are mentioned as they appear. As will be described later, TV signal strengths were measured at Sites A, B, C and at the top and bottom of each of the three turbines.

2.4 THE INTERFERENCE PHENOMENON

The rotating blades of a horizontal-axis WT can interfere with TV reception by producing video distortion. At a given distance from the WT, the interference increases with increasing frequency, and is, therefore, worse on the upper VHF channels than on the lower ones. It also decreases with increasing distance from the machine, but in the worst cases, it can still produce objectionable video distortion at distances up to a few kilometers. For ambient (primary) signals well above the noise level of the receiver, there is in general no significant dependence on the ambient field strength, and no audio distortion has been observed.

The interference is caused by the time-varying amplitude modulation of the received signal produced by the rotating blades. In a neighborhood of a WT, the signals scattered by the blades combine with the primary signal to create a form of time-varying multipath, thereby amplitude modulating the total received signal. The modulation waveform consists of sync pulses, and the pulses (whose width is inversely proportional to the electrical length of the blade) repeat at twice the rotation frequency of the blades. If sufficiently strong, these extraneous pulses can distort the received picture, whereas the audio information, being transmitted by frequency modulation, remains unaffected.

Table 2-2. Site Information

Site	Distance from WT No. 2	Direction from WT No. 2 (0° from N)	Approximate Height below WT No. 2 Axis
A	1600 m	200°	100 m
B	1600 m	120°	61 m
C	6096 m	247°	22 m

When the blades are stationary, the scattered signal may appear on the TV screen as a ghost whose position (separation) depends on the difference between the time delays suffered by the primary and scattered signals. A rotation of the blades then causes the ghost to fluctuate, and if the ghost is sufficiently strong, the resulting interference can be objectionable. In such cases, the received picture displays a horizontal jitter in synchronism with the blade rotation. As the interference increases, the entire (fuzzy) picture shows a pulsed brightening, and still larger interference can disrupt the TV receiver's vertical sync, causing the picture to roll over ("flip") or even break up. This type of interference occurs when the interfering signal reaches the receiver as a result of scattering, primarily specular, off the broad face of a blade, and this is called backward region interference. As the angle ϕ (see Figure 2-6) between the WT-transmitter and the WT-receiver direction increases, the separation of the ghost decreases, and a somewhat greater interference is then required to produce the same amount of video distortion. In the forward scattering region, when the WT is almost in line between the transmitter and the receiver, there is virtually no difference in the times of arrival of the primary and secondary signal. The ghost is then superimposed on the undistorted picture and the video interference appears as an intensity (brightness) fluctuation of the picture in synchronism with the blade rotation. In all cases, the amount of interference depends on the strength of the scattered signal relative to the primary one, and this decreases with increasing distance from the WT.

The backward region interference shows no significant dependence on the ambient signal strength and appears to be independent of the TV set if the signal is well above the noise level. Interference is observed only when a blade is positioned to direct the specularly reflected signal to the receiver. The azimuth and pitch angle of the blades are, therefore, key factors affecting the level of interference, and for any given transmitter and receiver locations, interference can occur only if the wind is such as to position the WT appropriately. In the forward region, however, the interference is less sensitive to the blade position but does depend on the ambient signal strength, and a receiver located in a low signal level area is more vulnerable to this type of interference.

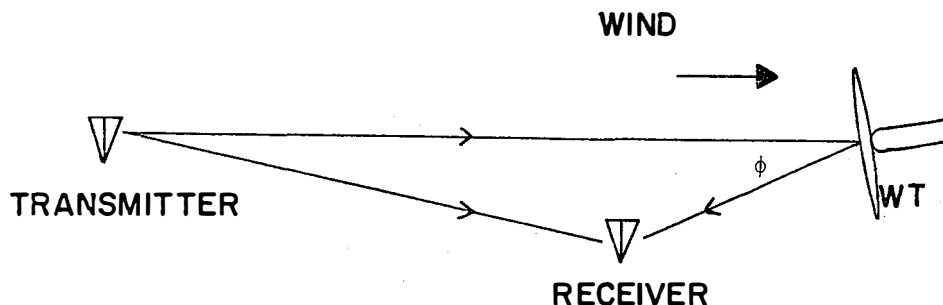


Figure 2-6. Geometry of the WT Blade Scattering

The amount of video distortion depends on the ratio of the scattered (perturbing) and ambient field strengths at the input to the receiver; i.e., on the modulation index m of the total received signal, and the modulation threshold m_0 is defined to be the largest value of m for which the distortion is still judged to be acceptable. The threshold is obviously somewhat subjective, but as a result of laboratory simulations [5,6,7], scale-model measurements [8], and field tests using the MOD-0 machines at Plum Brook [5,6] and on Block Island [2], it has been established as 0.15 for $\phi = 0$, increasing uniformly to 0.35 for $\phi \approx 180^\circ$ [4]. The latter value is for a strong ambient signal and could be as small as 0.15 in a low signal area. With the WT blades oriented to direct the maximum scattered signal to the receiver, the region where $m > m_0$ is defined as the interference zone.

On the assumption of a smooth spherical earth and an omnidirectional receiving antenna, a method has been developed [4] for calculating the interference zone of a WT for any given TV channel. The computation requires a knowledge of the effective length L_e and equivalent scattering area A_e of a WT blade. Figure 2-7 shows the resulting interference zone for TV Channel 11 with the transmitter 50 km for a MOD-1 WT [3]. We observed that the backward region corresponding to specular scattering off the blades is approximately a cardioid centered on the WT with its maximum pointing towards the transmitter. There is also a narrow lobe directed away from the transmitter produced by forward scattering. The shape of an interference zone is only weakly dependent on the transmitter distance and TV channel number, but its size increases markedly with increasing frequency (channel number).

Such computations have no direct relevance to the situation in Goodnoe Hills, where the hilly terrain has a pronounced effect on the level of interference

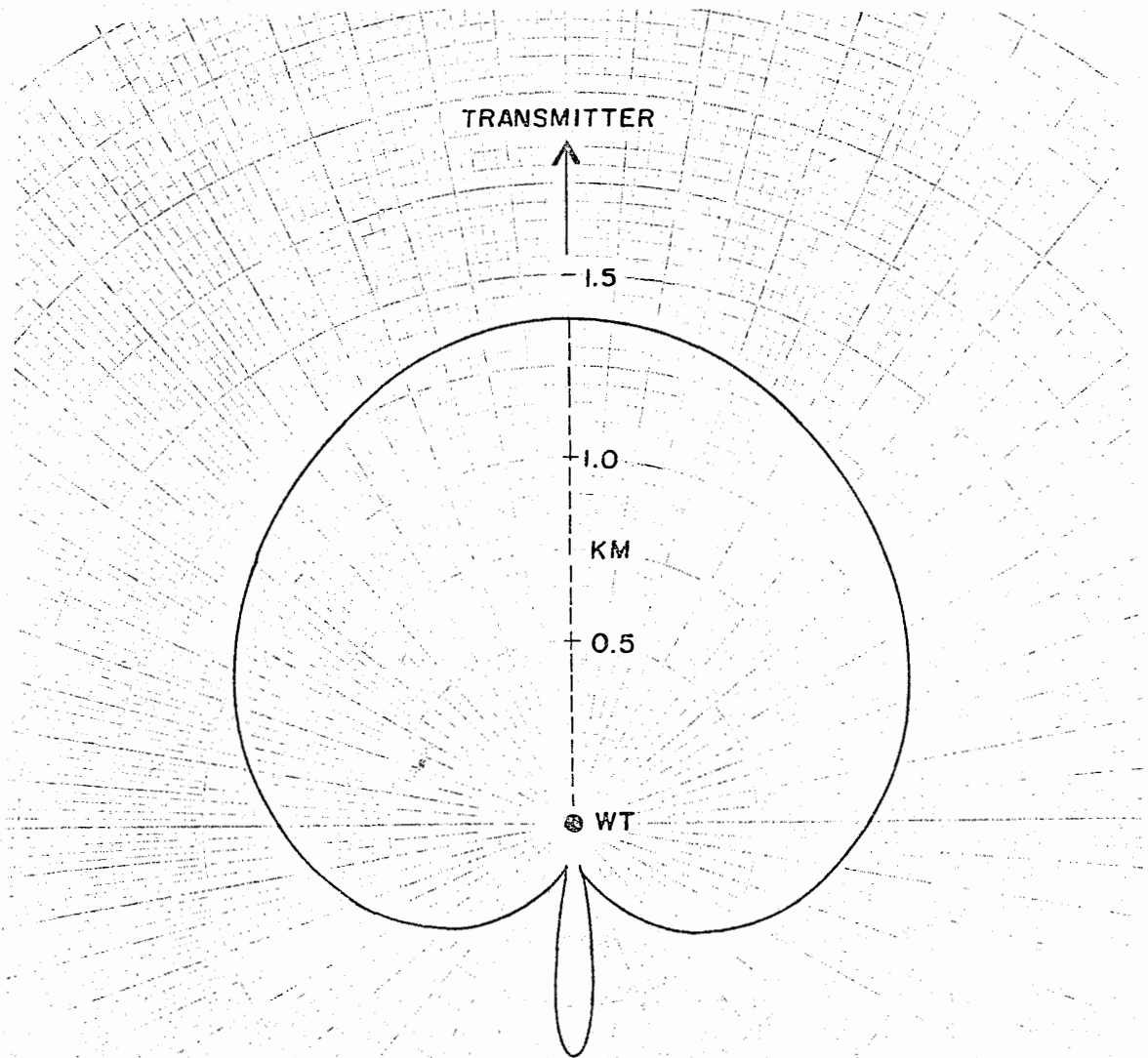


Figure 2-7. Theoretical Interference Zone for TV Channel 11 with Transmitter 50 km Away [3]
 ($A_e = 40 \text{ m}^2$, $L_e = 25 \text{ m}$.)

observed. In hilly country, homes tend to be on the lower slopes or in the valleys where, because of shadowing, the ambient field strengths may be less than if the terrain were flat. A WT, on the other hand, must be exposed to the winds and would naturally be placed on the higher ground, as in the present case. Because of the height-gain effect associated with the higher elevation, the illumination of the WT is stronger than it would be in flat terrain, thereby increasing the strength of the WT as a reradiating source. The net effect is to aggravate the interference, and to increase the distance from the WT at which the video distortion could be unacceptable.

However, there are also ameliorating factors. As previously remarked, the computation of an interference zone such as that in Figure 2-7 is based on the assumption that the WT azimuth is appropriate for directing the maximum scattered signal to the receiver, and if the winds necessary to operate the WT are generally from the SW or W, for example, some portions of the zone could experience relatively little interference. It is possible that the antenna can serve to discriminate against the unwanted interfering signal in the backward region.

If, in Figure 2-6, the main beam of the receiving antenna is pointed at the transmitter, the WT-scattered signal will be received via the side and back lobes of the antenna for most angles ϕ corresponding to the backward interference region, thereby reducing the observed interference. On the other hand, if the antenna is in the forward interference region of the WT, or that portion of the backward region where the direct and scattered signals are both received via the main beam, the antenna will lose most of its ability to provide discrimination.

With even a high-performance receiving antenna, the half-width of the main beam is much greater than the half-width of the forward peak of the interference zone. The discrimination that an antenna can provide is, therefore, limited by the pattern of the antenna and not by the nature of the interference zone, and since the discrimination is an important aspect of the present tests, it is convenient to define a modified (expanded) forward scattering region as that portion of the zone where the antenna will no longer produce any significant reduction in the interference. In the interests of simplicity and uniformity, we shall take the half-width of the modified forward scattering region to be 30° throughout the entire VHF band [3].

2.5 AVAILABLE TV SIGNALS

TV signals were received from two regions: Portland, Ore., and Pasco, Wash., which are located approximately 106 miles west and 80 miles northeast, respectively, of the WT site. Only VHF signals on TV Channels 2, 6, 8, and 12 were available from Portland; only UHF signals on Channels 19, 25, and 42 were available from Pasco. The ambient signal levels on all of the channels were generally low in the area. Typically, at the base of a WT, the received signal level on a given channel was about -70 dBm (\pm dBm) or lower, and so the received picture was poor. In addition, not all signals on all channels were available (for satisfactory reception) at all of the test sites. More details on this point are given later.

Figure 2-8 illustrates the geometrical orientation of the WT array site, the test sites and the directions of the TV stations at Portland and Pasco. We can see from Figure 2-8 that Sites A and C were in the forward region of the WTs for TV stations at Pasco and in the backward region for those at Portland; Site B was in the forward region for the Portland stations and in the backward region for the Pasco Stations.

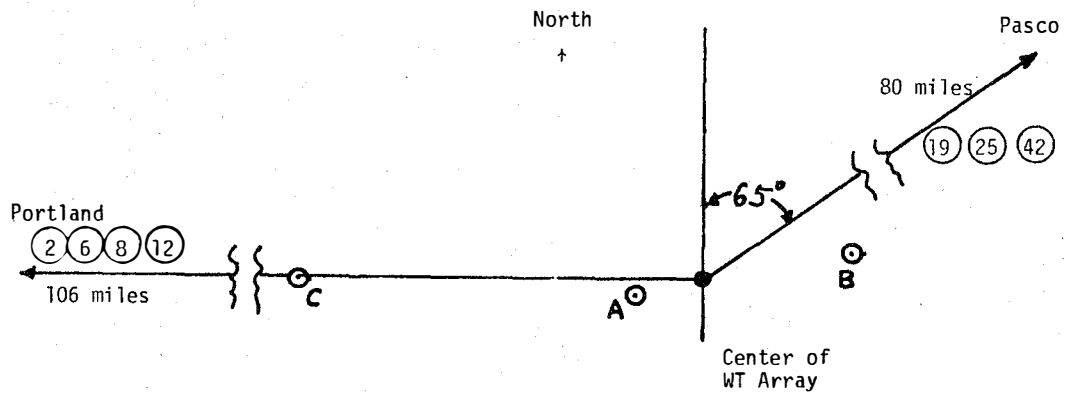


Figure 2-8. Location of the Available TV Signal Transmitters with Respect to the WT Array and the Test Sites. Circled numbers indicate TV channel numbers.

SECTION 3.0

TEST EQUIPMENT AND PROCEDURES

3.1 EQUIPMENT

In general, the equipment used to perform the measurements was similar to that for measurements made at other WT sites [2,3]. A schematic block diagram of the system is shown in Figure 3-1, which includes only those components pertinent to the data collection. With any given TV transmission, a portion of the signal is scattered by the WT(s) and this, together with the desired (direct) signal, was picked up by an antenna and fed to an RFI receiver and a TV receiver. The receiving antenna, which is described later, was a commercially available directional antenna located 38.5 feet above the ground.

The appropriate output for the RFI receiver was connected to a chart recorder which provided a record on paper tape for later evaluation. The combination of the RFI receiver and the recorder was used to measure the ambient levels of the video and audio signals when the WTs were not in operation, and to record the total signal received as a function of time, including any modulation produced by the scattering of the operating WTs. The general quality of the ambient TV reception and the existence of any WT-produced video distortion were observed on the TV screen and the video recorder was employed whenever it was felt desirable to record the program. All the test instruments fitted comfortably inside a van (supplied by BPA). The receiving antenna and its associated tower and rotor assemblies were installed on the van in a demountable fashion. The test equipment was powered from a portable 60-Hz supply installed in the van. The van equipped in this manner served as a mobile laboratory and was used as such throughout the entire test program. For future reference, the following is a list of the major equipment included in the mobile laboratory:

1. RFI receiver (Singer Model NM37/59)
2. X-Y recorder (Brinkman Model 2551)
3. Video recorder (Sony Model 2800)
4. Television receiver (Sony 12-inch screen)
5. Antenna on tower
6. Antenna rotor
7. Walkie-talkie (1)
8. Portable power supply
9. Van

Note that during the present tests we used an RFI receiver instead of the Hewlett-Packard spectrum analyzer that was employed during our previous tests [2,3]. This RFI receiver has a noise level which is 25 dB lower than the spectrum analyzer mentioned above. For example, the minimum detectable signals for the receiver and the spectrum analyzer are -105 and -80 dBm, respectively. Thus, the use of the RFI receiver was an advantage during the

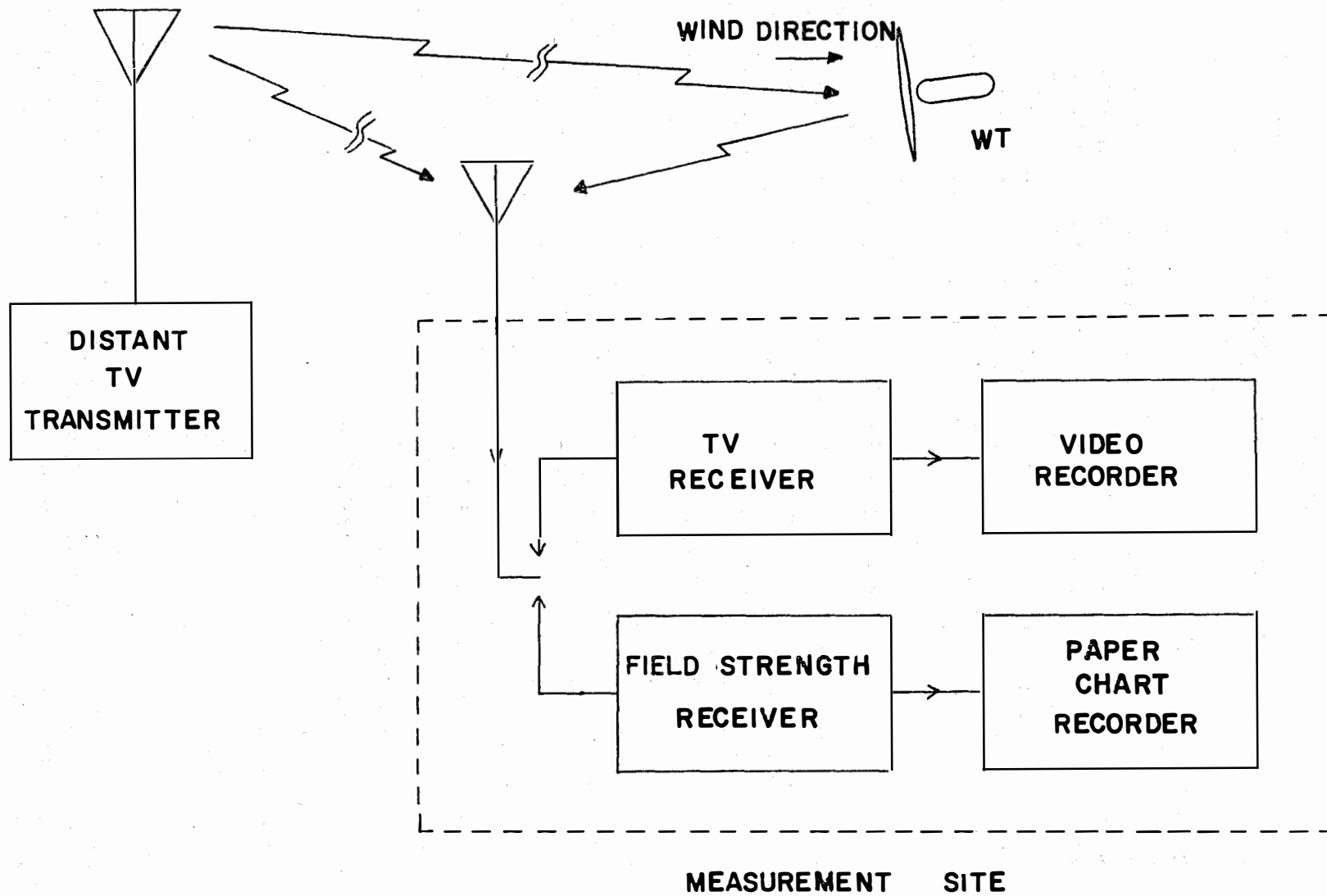


Figure 3-1. Schematic Block Diagram of the Measurement System

measurements in the Goodnoe Hills area where ambient signal levels generally were low.

3.2 THE RECEIVING ANTENNAS

The following three directional receiving antennas were used during various phases of the test program:

- (1) Winegard antenna (50-216 MHz) (Model CH 3400) used for VHF channels.
- (2) Fairchild logconical spiral antenna (200-1000 MHz) (Model LCA-25) used for UHF channels.
- (3) Singer broadband biconical antenna (20-200 MHz) (Model 94455-1) used for VHF channels.

At remote test Sites A, B, and C, test data on VHF and UHF channels were collected by using the Winegard and logconical antennas, respectively. At the WT sites, biconical and logconical antennas were used to collect data on VHF and UHF channels. At the wind turbine sites it was necessary to measure the ambient signal strengths at the base of the three turbines and at the top of WT No. 2. For the latter, the use of the Winegard antenna was considered to be mechanically disadvantageous. The relevant gain characteristics of the Winegard antenna relative to the biconical antenna are given in Table 3-1.

3.3 TYPES OF MEASUREMENT

At each test site, some or all of the following types of measurements were performed for every TV channel of interest.

- (i) Received Signal Strength: With the WT stationary, the strength of the received signal was measured by rotating the mainbeam of the receiving antenna until the output was maximum. Tuning the receiver through the TV channel band of frequencies caused both video and audio signal strengths on each channel to be obtained.
- (ii) Antenna Response: In some cases, as the antenna was rotated, the output of the receiver tuned to the audio carrier frequency was recorded as a function of time, with and without the WT blades rotating. These measurements served to determine (a) the horizontal plane pattern of the antenna in an actual test environment, (b) the effect of the WTs on the received signals, and (c) the amount of signal modulation produced by the operating turbine(s).
- (iii) Blade Scattering: With the blades of a specific machine (e.g., WT No. 2) locked in a desired position (horizontal or vertical) and their pitch set for maximum power, the WT was yawed in azimuth through 360°. Measuring the TV signal received with the antenna pointed at the TV transmitter and then at the WT enabled us to determine the maximum blade-scattered signal. During these static tests, the other two turbines (WT No. 1 and WT No. 3) were kept stationary.

Table 3-1. Gain Characteristics of the Winegard Antenna Relative to the Biconical Antenna

Channel No.	Gain Relative to the Biconical Antenna	
	Video	Audio
2	9.0 dB	9.5 dB
6	9.0 dB	8.5 dB
8	9.0 dB	6.5 dB
12	10.0 dB	12.0 dB

- (iv) TV Interference: These dynamic tests required the WT blades to be rotating. The antenna beam was positioned to receive the maximum signal as a normal TV reception (generally when the beam was directed at the TV transmitter), and the receiver was tuned to the audio carrier frequency. Its output was then recorded as a function of time, and the received picture on the TV screen was observed for any video distortion. In a few instances, the measurements were repeated with the antenna beam pointed toward the WTs to simulate the worst possible situation of a mispositioned antenna. Dynamic data were collected when the WTs operated both singly and in an array.

As we mentioned in Section 2.4, the signal scattered by a rotating blade combines with the direct signal to produce an amplitude modulated signal at the inputs to the RFI and TV receivers. Thus, as a function of time, the output of the RFI receiver varies above and below the ambient signal level, and it is conventional to quote the total variation (Δ) of the received signal amplitude in dB, from which the amplitude modulation index (m) can be obtained using the relationship $\Delta \approx 20 \log_{10} [(1 + m)/(1 - m)]$. Usually, a total signal variation greater than or equal to 2.6 dB ($m \geq 0.15$) causes unacceptable video distortion for backward region interference [4,5,7]; however, we should mention that barely visible but acceptable distortion may occur even for $\Delta < \Delta_0 = 2.6$ dB. For the forward region interference, the corresponding value of Δ_0 is larger, and can be as large as 6.5 dB ($m \approx 0.35$) [3] for ambient signals on the order of -60 dBm but smaller for weaker ambient signals.

SECTION 4.0

MEASURED AMBIENT SIGNAL STRENGTHS

The quality of TV reception at any place depends on the signal-to-noise ratio of the receiver, on the receiving antenna used, and, obviously, on the TV signal's strength. To determine the quality that is possible in the Goodnoe Hills area, the ambient signal strengths were measured at all of the test sites on all of the available TV channels.

4.1 RECEIVED SIGNAL STRENGTH AND QUALITY OF RECEPTION

To provide good video reproduction, the received video signal should produce a minimum of 1.0 mV rms across the input terminals of a TV receiver presenting an impedance of 75 ohms [9], and if the signal produces only 0.2 mV, the picture will be snowy and of generally poor quality. The corresponding video signal powers P_v at the input terminals of the receiver are 1.3×10^{-5} and 5.3×10^{-7} mW; i.e., -49 and -63 dBm, respectively, where dBm denotes decibels above one milliwatt. Thus, if $P_v \geq -49$ dBm, good reception is possible, but as P_v decreases below -49 dBm, the reception will become increasingly poor (snowy); and for $P_v < -63$ dBm, the reception will be extremely poor to unacceptable. During our previous measurements of P_v [3], simultaneous observations of the picture quality obtained with the TV receiver were generally consistent with these criteria.

As mentioned in Section 3.3, for measurements of WT interference the receiver is tuned to the TV channel audio carrier frequency. Since the relevant ambient signal strength is the received audio signal power P_a , it is convenient to express the criteria for quality of reception in terms of this parameter. It has been found that the quality of reception is approximately related to P_a as follows [3]:

$P_a \geq -56$ dBm	Good reception
$-56 > P_a \geq -70$ dBm	Poor (snowy) reception
$P_a < -70$ dBm	Extremely poor (unacceptable) reception.

These imply that, on the average $(P_a/P_v) = -7$ dB.

The above criteria given in dBm have been found very convenient to use when measurements are carried out with a spectrum analyzer which is calibrated in dBm [2,3]. During the present measurements, we have used an RFI receiver which yields the received signal (field) strengths in dB μ V (i.e., decibels above one microvolt). For the present receiver, the dBm criteria given above can be converted into dB μ V criteria using the relationship dB μ V = dBm + 107 and are as follows:

$E_a \geq 51$ dB μ V	Good reception
$51 > E_a \geq 37$ dB μ V	Poor (snowy) reception

$$E_a < 37 \text{ dB}\mu\text{V}$$

Extremely poor (unacceptable) reception.

4.2 SIGNAL STRENGTHS AT THE WT ARRAY SITE

Signal strengths were measured at the bases of the three WT towers and on top of the nacelle of WT No. 2. Measurements at the base of a turbine were carried out by using an appropriate receiving antenna located 38.5 ft above ground. For the latter measurements, the receiving antenna (logconical or biconical) was mounted on a six-ft metallic pole placed vertically on the roof of the nacelle at the end farthest from the blades. The turbine blades were set in a horizontal position and the axis of the WT placed on the north-south line so that there would be little or no interference due to the blades for signals being received from Portland or Pasco. The antenna was connected to the RFI receiver using a 250-ft length of coaxial cable, and the 6-dB (approximately) attenuation that this introduced has been taken into account in quoting the signal strengths that were measured. The desired results were obtained by yawing the WT in azimuth to receive the maximum signal on each channel.

Signals on VHF TV Channels 2, 6, 8, and 12 and UHF TV Channels 19, 25, and 42 were available at the WT array site. Biconical and logconical receiving antennas were used to receive the VHF and UHF signals, respectively. The video and audio carrier field strengths on the channels of interest, obtained at the bases of WT Nos. 1 and 3, are given in Table 4-1. The corresponding results obtained at the base and on top of WT No. 2 are shown in Table 4-2.

Received signal levels shown in Tables 4-1 and 4-2 indicate that they would generally provide a poor to unacceptable quality of reception with similar receiving antennas. Signals on all of the channels received at the bases of WT Nos. 1 and 2 were generally of the same order of magnitude; VHF and UHF signals received at the base of WT No. 3 were generally larger and smaller,

Table 4-1. Received Field Strengths at the Bases of WT Nos. 1 and 3 with the Receiving Antenna Located 38.5 ft Above the Ground

TV Channel Number	WT No. 1		WT No. 3	
	E_v dB μ V	dB μ V	dB μ V	dB μ V
2	32.0	34.0	38.0	38.0
6	33.0	29.0	39.0	36.0
8	25.0	21.5	41.0	35.0
12	28.0	26.5	38.0	34.0
19	42.0	39.0	22.0	20.0
25	41.5	34.0	17.0	16.0
42	37.0	36.0	13.0	8.0

Table 4-2. Received Field Strengths at the Base and on Top of WT No. 2

TV Channel Number	Base of the WT		Top of the WR	
	E_v dB μ V	E_a dB μ V	E_v dB μ V	E_a dB μ V
2	27.0	27.0	34.0	30.0
6	45.4	41.0	47.5	42.0
8	29.0	20.0	35.0	27.0
12	29.5	23.0	32.0	31.0
19	42.0	38.5	46.0	46.0
25	41.0	37.0	46.5	39.0
42	41.5	36.5	47.0	45.0

respectively, than those at the other two turbines. Signals received on top of WT No. 2 were found to be slightly larger than those at the base. These variations in received signal strengths in various cases are not well understood; this may be due to the hilly nature of the terrain and the TV transmitters of interest being far away.

4.3 SIGNAL STRENGTHS AT SITES A, B, AND C

Field strengths measured with the biconical (for VHF channels) and the logconical (for UHF channels) antennas located 38.5 ft above ground at the three remote test sites are listed in Table 4-3, which indicates that the quality of reception on all of the TV channels at the three sites is extremely poor to unacceptable. In a few cases, we have used the Winegard antenna to receive the VHF signals; this antenna has a higher gain than the biconical antenna

Table 4-3. Field Strengths at the Remote Test Sites Received with Biconical (VHF) and Logconical (UHF) Antennas Located 38.5 ft Above the Ground

Site A			Site B			Site C		
TV Channel Number	E_v dB μ V	E_a dB μ V	TV Channel Number	E_v dB μ V	E_a dB μ V	TV Channel Number	E_v dB μ V	E_a dB μ V
2	32.0	31.5	2	31.0	27.5	2	21.0	20.0
6	35.0	29.5	6	26.5	22.5	6	31.0	26.5
8	40.0	36.5	8	27.0	24.0	8	12.0	14.0
12	39.0	31.5	12	28.0	19.5	12	6.0	4.0
19	27.5	24.5	19	42.5	40.5	19	15.0	7.5
25	25.0	18.0	25	44.5	40.5	25	12.0	6.5
42	13.5	13.5	42	39.5	37.0	42	10.0	6.0

(see Table 3-1) and generally provided received signals about 9 to 12 dB stronger. However, even with the use of the high-gain antenna, the reception on VHF channels at the three sites was considered to be poor to unacceptable.

4.4 CONCLUSIONS

It is evident from the above results that (i) at the WT array site and its surrounding area, the field strengths of all of the available TV channels are weak. The quality of TV reception in the area is generally poor to unacceptable, and even with the WTs stationary and a high-performance antenna such as the Winegard, it did not become good. (ii) Considerable variations in the field strengths were observed at the three remote test sites, and also at the bases of the three turbines. The weak nature of the received signals and their variations between sites are attributed to the combined effects of the TV transmitters being far away and the rolling hills in the surrounding area.

SECTION 5.0

BLADE SCATTERING (STATIC TESTS)

5.1 COMMENTS ON THE BLADE SCATTERING PARAMETERS

The interference produced by the rotating blades of a WT is directly proportional to the scattering from a blade [4-7]. It has been shown in Ref. [4] that a knowledge of the equivalent scattering area (A_e) and equivalent length (L_1) of a blade is required to determine the interference distance and interference zone of a given WT. For the rectangular plate model of the WT blade, which has been found useful in our previous studies [2,5], the equivalent scattering area of a blade is defined as

$$A_e = L_1 L_2 ,$$

where L_1 and L_2 are the equivalent length and width, respectively, of the blade.

The scattering parameters of MOD-0, MOD-0A and MOD-1 blades have been determined from laboratory (scale-model) and full-scale scattering measurements reported earlier [3,5]. Similar information about the MOD-2 blades was obtained in the laboratory using the results of laboratory scale model measurements [10] carried out in our anechoic chamber. No confirmation of these results by means of full-scale measurements has been available until now.

The MOD-2 blade appears to have five distinct sections: a center section, two outer sections, and two tip sections. The projected areas of the center, outer, and tip sections are approximately 88, 60, and 26 m², respectively, leading to a total blade projected (physical) area $A_p = 260$ m², of which the tips make up 52 m². The overall length is 91 m, but only 64 m if the tips are excluded. Laboratory measurements at 3.034 GHz, carried out with a 1:100 scale model of a MOD-2 blade, yielded the following results [8]:

$$A_e = 184 \text{ m}^2 , L_1 = 84 \text{ m} .$$

Under full power conditions, the tips are usually twisted (pitch $\neq 0$), and it was found that the tips contributed very little (or nothing) to the peak scattering return. Therefore, it appears that the results for the tips twisted (or removed) are appropriate to the practical situation. It was found, then, that

$$A_e = 140 \text{ m}^2 , L_1 = 63 \text{ m} ,$$

which implies a scattering efficiency $\eta = 0.67$ (note: $A_e = \eta A_p$) which was identical to the efficiency for the MOD-0 or MOD-1 blade [3,5]. The scattering parameters $A_e = 140$ m² and $L_1 = 63$ m, obtained under the assumption of negligible return from the tips, have been used to calculate the interference distance and zones of a MOD-2 WT [4].

The present program provided an opportunity to check these values experimentally by taking static measurements of the blade scattering at a few sites. In the following sections, we discuss the results and describe how the equivalent scattering parameters have been determined from the measured data.

5.2 PROCEDURE

As we mentioned in Section 3.3, the blades of the WT were maintained at zero-degree pitch (full power condition) and locked in a horizontal position throughout these tests. For convenience, only WT No. 2 was used during the tests. Using local TV transmitters as the rf sources, and with the receiving antenna directed at the WT, the received signals were recorded in dB μ V as functions of time as the machine was yawed in azimuth. Information about the yaw position (i.e., the position of the blade with respect to the receiving antenna) was received from WT personnel and was inserted later on the signal record. This information was then used to obtain the nacelle (or blade) pointing direction, in effect, to produce a plot of the received scattered signal vs. blade rotation angle.

5.3 RESULTS

Data were recorded on Channel 6 at Site A, and on Channels 6 and 8 at Site C; both sites were such that backscattered signals were obtained. Figures 5-1, 5-2, and 5-3 show the portions of the received signals vs. time (or blade rotation angle), and showing the scattered signals received from the front side of the blade (i.e., the blade facing the test site). Although the scattered signals were strongest at Site A, the scattering patterns were clearly identifiable in all three cases.

Additional tests were conducted with the blades vertically oriented; however, we were not able to detect appreciable scattered signals during these measurements. It is believed that this was because (i) the scattering pattern (in the vertical plane) of the vertically oriented blade is very narrow, and its maximum is generally directed in a direction normal to its face; and (ii) the teetering mechanism (beyond control) may direct the maximum direction upward. Because the receiving sites are below the phase center of the blade, the combination of the two effects above was responsible for the reception of weak scattered signals when the blades were vertical.

For the data analysis discussed later, we would also need the ambient signal strengths (on Channels 6 and 8) at the phase center of the blade of WT No. 2 (i.e., on top of it). These ambient field strengths measured with a logconical receiving antenna were given in Table 4-2. The static measurements at Sites A and C were conducted with the Winegard as the receiving antenna. Therefore, it is necessary to obtain the ambient field strengths on top of WT No. 2 when a similar antenna is used there to receive the signals. With the gain characteristics of the Winegard antenna (see Table 3-1), the results given in Table 4-2 were used to obtain the required ambient signal strengths.

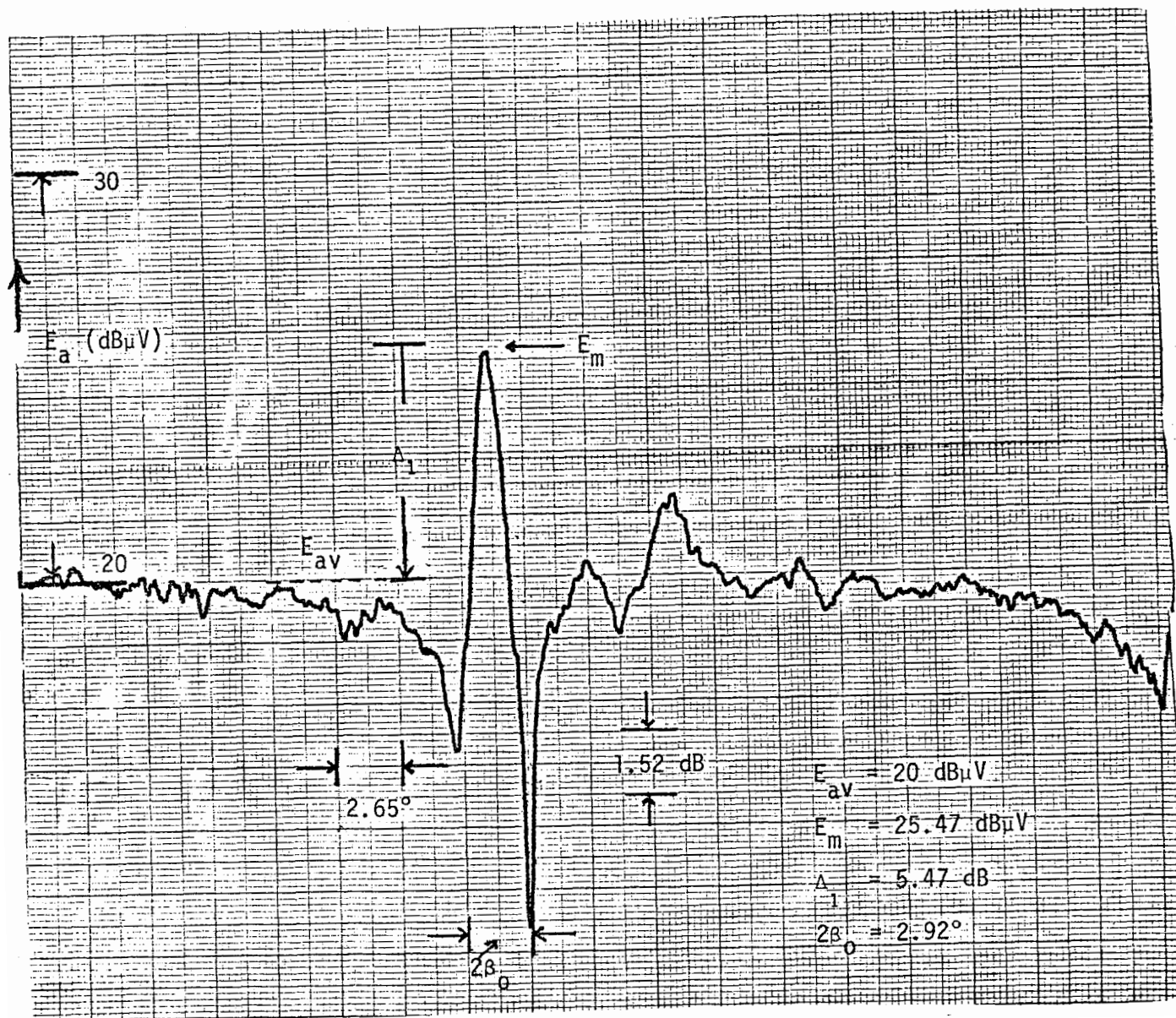


Figure 5-1. E_a (dB μ V) vs. WT No. 2 Yaw Angle (blades horizontal) on Channel 6, Obtained at Site A
($\beta = 0^\circ$ at $E_a = E_m$.)

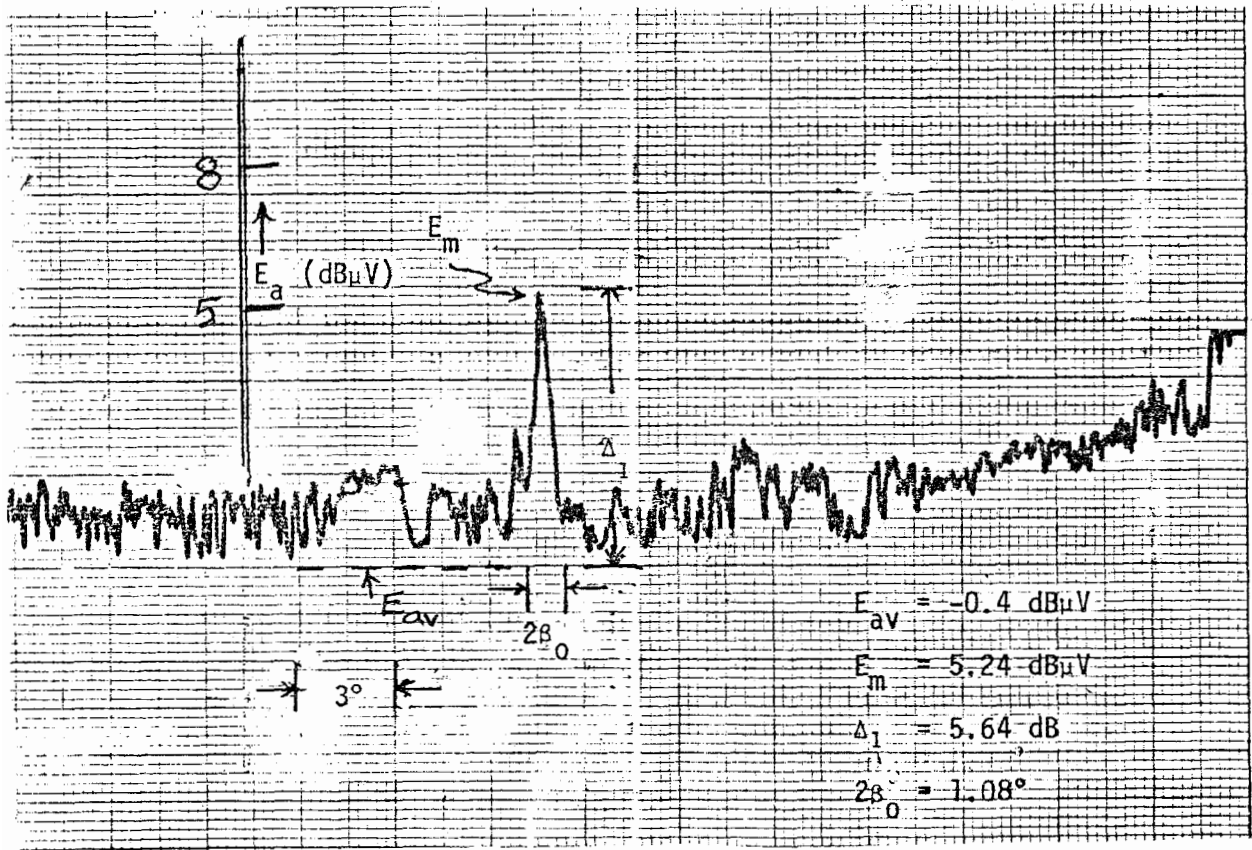


Figure 5-2. E_a (dB μ V) vs. WT No. 2 Yaw Angle (blades horizontal) on Channel 8, Obtained at Site C
 ($\beta = 0^\circ$ at $E_a = E_m$.)

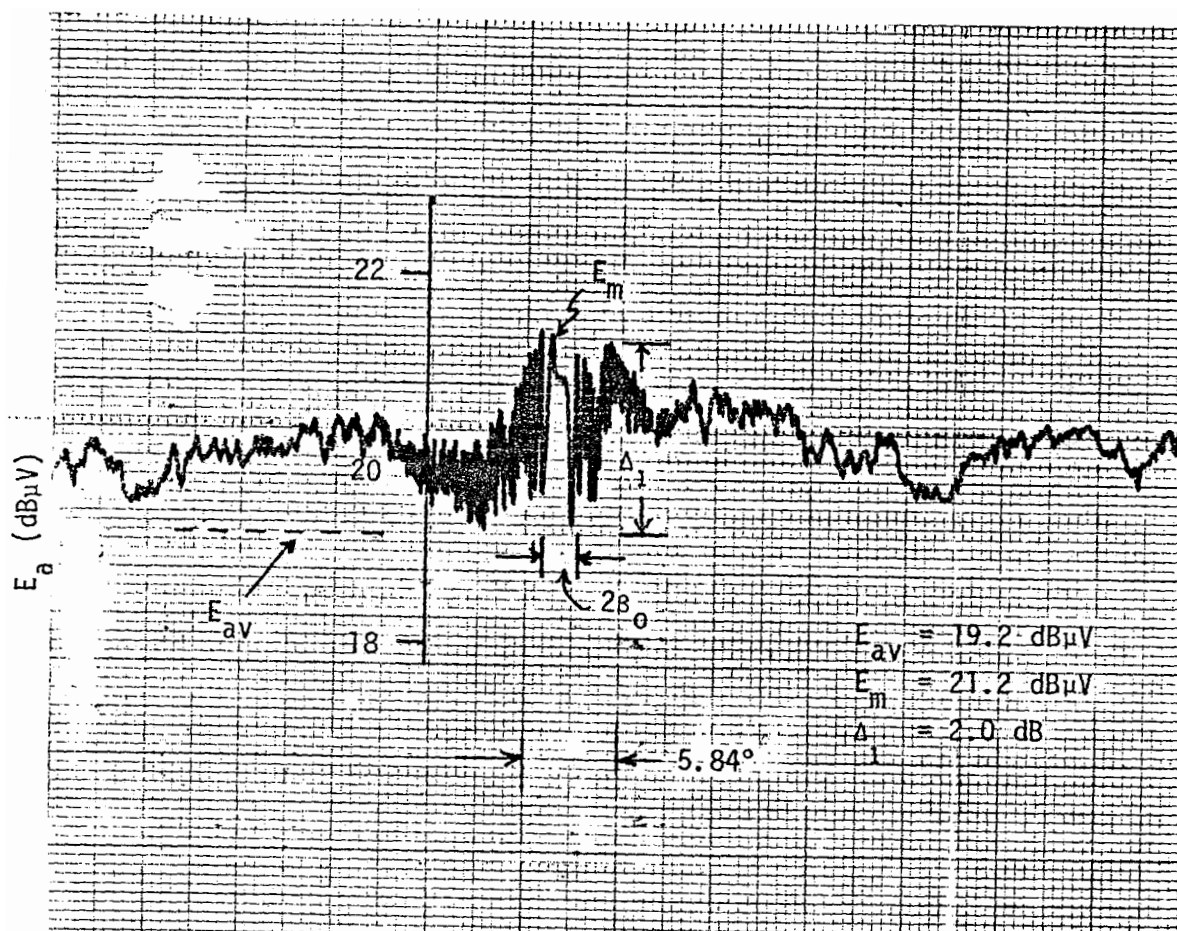


Figure 5-3. E_a (dB μ V) vs. WT No. 2 Yaw Angle (blades horizontal) on Channel 6, Obtained at Site C
 ($\beta = 0^\circ$ at $E_a = E_m$.)

5.4 THEORETICAL EXPRESSIONS

Before analyzing the measured data to determine the scattering parameters of the blade, it is appropriate to discuss the geometry involved and give the required theoretical expressions which were derived in our earlier report [3]. Figure 5-4 shows a horizontal plane view of the geometry where R and B represent the receiving point and the phase center of the blades, respectively. The bistatic angle between the transmitter and the receiver with respect to the blade center is represented by the angle $2\phi_0$ in Figure 5-4. The blade rotation angle is represented by β such that $\beta = 0^\circ$ (shown in Figure 5-4) corresponds to blade orientation when R receives signals specularly scattered off the blade. The corresponding elevation plane view of the geometry is shown in Figure 5-5, where α represents the elevation angle of the blade center B as viewed from R. With the above conventions, the received signal data given in Figures 5-1 through 5-3 may be interpreted as the received field strength E vs. the blade rotation angle β , with $\beta = 0^\circ$ yielding the maximum scattering return. We have identified the following parameters in Figure 5-1:

E_{av} = average or ambient level

E_m = maximum level

$\Delta = E_m - E_{av}$ = maximum deviation from the ambient level

$2\beta_0$ = width in degrees of the main scattering lobe between the first nulls.

$$A_e \approx \frac{m\lambda r}{\frac{E_a(B)}{E_{av}} \cos \phi_0 \text{sinc}_1 \text{sinc}_2} \quad (5-1)$$

$$L_1 \approx \frac{0.5}{\cos \phi_0 \sin \beta_0}, \quad (5-2)$$

where

$$\text{sinc}_1 = \frac{\sin \pi x_1}{\pi x_1}, \quad \text{sinc}_2 = \frac{\sin \pi x_2}{\pi x_2}, \quad (5-3)$$

$$x_1 = \frac{L_1}{\lambda} \{(1 - \cos \alpha) \sin \phi_0\}, \quad (5-4)$$

$$x_2 = \frac{L_2}{\lambda} \sin \alpha, \quad (5-5)$$

with

λ = wavelength of the audio carrier signals

$E_a(B)$ = audio carrier signal strength at B

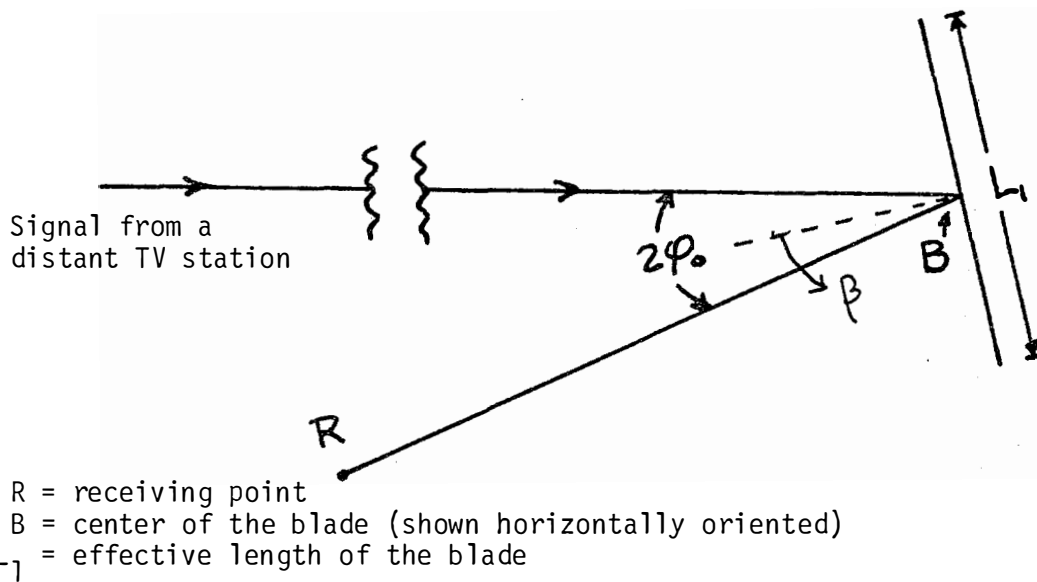


Figure 5-4. Horizontal (or Azimuthal) Plane Geometry of the Blade, the Receiver, the Incident and Scattered Field Directions

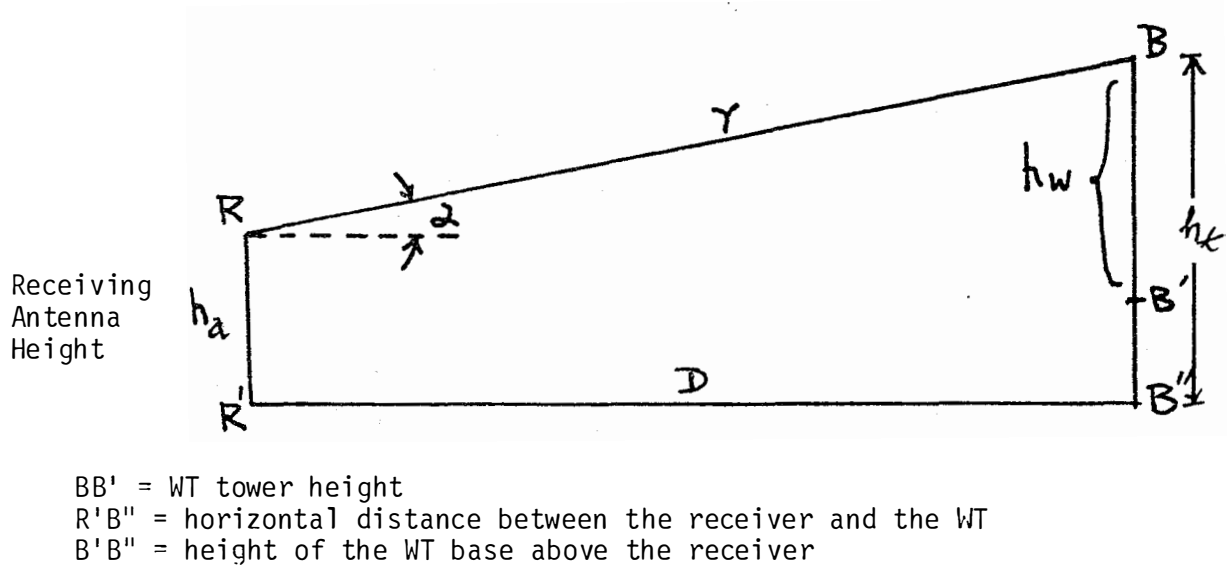


Figure 5-5. Elevation Plane Geometry of the Blade, the Receiver, the Incident and Scattered Field Directions

r = distance between B and R

L_1, L_2 = the equivalent length and width of the blade (i.e., $A_e = L_1 L_2$)

and the other parameters are as defined earlier.

The expressions given above are in terms of measured parameters and will be used in the following section to determine the required blade scattering parameters. We should mention here that because of the rugged nature of the terrain surrounding the WT, the effects of ground reflection have been neglected in obtaining Eqs. 5-1 and 5-2.

5.5 DATA ANALYSIS

The equivalent scattering parameters for the MOD-2 blade can be determined from the data presented in Section 5.3 by applying the theoretical relations given in Section 5.4. The symbols used are defined earlier, and we show the detailed calculations for one case only.

(i) Site A, Channel 6. Known parameters:

λ (audio carrier wavelength)	= 3.42 m
elevation (above sea level) of the receiving site (i.e., R' in Figure 5-5)	= 744 m
height of the receiving antenna above ground h_a (in Figure 5-5)	= 11.7 m
elevation of WT No. 2 base (i.e., of B' in Figure 5-5)	= 783 m
WT No. 2 tower height h_w (i.e., BB' in Figure 5-5)	= 61 m
horizontal distance between the WT and the receiving site (i.e., R'B" in Figure 5-5)	D = 1600 m
bistatic angle between the transmitter and the receiver (Figure 5-4)	$2\phi_0 = 70^\circ$

Measured parameters (see Figure 5-1):

$$E_{av} = 20 \text{ dB}\mu\text{V}$$

$$E_m = 25.47 \text{ dB}\mu\text{V}$$

$$\Delta_1 = 5.47 \text{ dB}$$

$$2\beta_0 = 2.92^\circ$$

$$m = \text{Antilog} (\Delta_1/20) - 1 = 0.88$$

Using Tables 4-2 and 3-1, obtain $E_a(B)$ as

$$E_a(B) = 42 \text{ (Table 4-2)} + 8.5 \text{ (Table 3-1)} = 50.5 \text{ dB}\mu\text{V.}$$

Calculations:

$$h_t = h_w + (783 - 744) = 61 + 39 = 100 \text{ m}$$

$$r = [D^2 + (h_t - h_a)^2]^{1/2} \approx 1600 \text{ m}$$

$$\alpha = \tan^{-1} \frac{h_t - h_a}{D} = \tan^{-1} \frac{100 - 11.7}{1600} \approx 3.16^\circ$$

$$\cos \phi_o = 0.8192, \cos \alpha = 0.9985, \sin \beta_o = 0.0255$$

$$\frac{L_1}{\lambda} = \frac{0.5}{\cos \phi_o \sin \beta_o} = \frac{0.5}{0.8192 \times 0.0255} = \underline{23.9}$$

$$L_1 = 23.9 \times 3.42 = \underline{81.7 \text{ m}}$$

$$x_1 = (1 - \cos \alpha) \frac{\pi L_1}{\lambda} \sin \phi_o \approx 6.46 \times 10^{-2}$$

$$\text{sinc}_1 = \frac{\sin \pi x_1}{\pi x_1} \approx 1.0$$

$$\text{since } L_2 \ll L_1, \text{ sinc}_2 \approx 1.0$$

$$\frac{E_a(B)}{E_{av}} = 50.5 - 20 = 30.5 \text{ dB} = 33.5$$

$$A_e = \frac{0.88 \times 3.42 \times 1600}{33.5 \times 0.8192 \times 0.9985} = 175.73 \approx \underline{176 \text{ m}^2}.$$

(ii) Site C

(a) Channel 8.

$$\lambda = 1.62 \text{ m}, h_a = 11.7 \text{ m}, h_t = 222 \text{ m}, 2\phi_o = 23^\circ, 2\beta_o = 1.08^\circ$$

$$r \approx D = 6096 \text{ m}$$

$$\alpha = 1.98^\circ, \cos \alpha \approx 1, \cos \phi_o = 0.9749, \sin \beta_o = 0.0094$$

$$E_{av} = -0.4 \text{ dB}\mu\text{V}, E_m = 5.24 \text{ dB}\mu\text{V} \quad E_a(B) = 27 + 6.5 = 33.5 \text{ dB}\mu\text{V}$$

$$\frac{E_a(B)}{E_{av}} = 49.5, \Delta_1 = 5.64 \text{ dB}, m = 0.91$$

$$\frac{L_1}{\lambda} = 54.3, L_1 = 87.9 = \underline{88 \text{ m}}$$

$$A_e = 186.22 = \underline{186 \text{ m}^2}$$

(b) Channel 6. Signals were received with a Yagi antenna. The received ambient signal at B, therefore, was adjusted to correspond to the same antenna.

$$\lambda = 3.42, \beta_0 = 1.17^\circ, \phi_0 = 11.5^\circ$$

$$E_a(B) = 48.5 \text{ dB}\mu\text{V}, E_m = 21.2 \text{ dB}\mu\text{V}$$

$$E_{av} = 19.2, \frac{E_a(B)}{E_{av}} = 29.2, \Delta_1 = 2.0, m = 0.26 .$$

Other parameters are the same as those in (ii)(a):

$$\frac{L_1}{\lambda} = \underline{25.0}, L = 85.5 = \underline{86 \text{ m}}$$

$$A_e = 190.42 = \underline{190 \text{ m}^2} .$$

For future reference, the scattering parameters for the MOD-2 blade obtained from the static measurements are presented in Table 5-1. As we mentioned earlier, the corresponding values obtained from laboratory scale-model measurements are $A_e = 184 \text{ m}^2$, $L_1 = 84 \text{ m}$. The agreement between the results of the two measurements is excellent.

Table 5-1. Equivalent Scattering Parameters for the MOD-2 Blade Obtained from Full-Scale Measurements

Site	Distance from WT (m)	TV Channel No.	Wavelength (m)	A_{e2} (m^2)	L_1 (m)
A	1600	6	3.42	176	82
C	6096	8	1.62	186	88
C	6096	6	3.42	190	86

5.6 DISCUSSION

Based on the measurements carried out on TV Channel 6 at Site A, and on TV Channels 6 and 8 at Site C, the following observations can be made: (i) The average of the measured values for the equivalent scattering area A_e and length L_1 of the front face of the MOD-2 blade with its pitch adjusted for maximum power are in excellent agreement with the values obtained from laboratory scale-model measurements. The tests provide confidence in the validity of the theoretical model and the scale-model measurements. (ii) As mentioned in Section 5.1, it is recommended, therefore, that in practical situations when the pitch is not adjusted for maximum power $A_e = 140 \text{ m}^2$ and $L_1 = 63 \text{ m}$ should be used for the scattering parameters of the MOD-2 blade.

SERIO 

SECTION 6.0

TELEVISION INTERFERENCE MEASUREMENTS (DYNAMIC TESTS)

The nature and degree of television interference caused by the operation WTs were determined by carrying out dynamic measurements at test Sites A, B, and C. As indicated earlier (Section 3.3), the tests involved the measurement of the received signal vs. time for the antenna beam pointed toward the WT array and, on a few occasions, at the TV transmitter. Whenever it was felt desirable, the quality of TV reception was also simultaneously monitored using the TV receiver.

Dynamic data were collected with the turbine blades rotating at 17.5 rpm and for the wind conditions available at the time of the tests. During the time period of the measurements, wind generally was coming from the west, thereby causing the axes of rotation of the operating WTs to line up along the east-west line. During TVI measurements at Sites A and C, this generally provided backward and forward zone conditions, on TV channels originating from Portland and Pasco, respectively (see Figure 2-8).

Typically, data were collected with one WT operating at first, then two. Normally these results were obtained with WTs No. 2 and No. 3. Only in a few cases were we able to collect some data with all three machines operating. In the following sections, we give the results of the dynamic measurements conducted using the available TV channels at the three test sites and for various operating conditions of the WTs.

6.1 SITE A

Ambient signals on all of the available TV channels at this site were very weak (see Table 4-3) and generally provided extremely poor-to-unacceptable reception under normal conditions. Of the three UHF TV channels, Channel 19 had the strongest ambient signals; therefore, we selected this channel for collecting the initial set of dynamic data. As mentioned earlier, Test Site A was in the forward interference zone of the WTs for the reception of Channel 19. Results obtained under various dynamic conditions are shown in Figures 6-1 through 6-3.

Figure 6-1 refers to the results obtained with only WT No. 2 operating; the average spacing between the pulses is about half the rotation period (1.72 s) of the blades rotating at 17.5 rpm. The total signal variation caused by the pulses is $\Delta \approx 7.4$ dB, which produced considerable video interference; in fact, because the ambient signals are extremely low, the TV interference consisted of the received pictures fading in and out of the TV screen in synchronism with these pulses.

Similar results obtained with WTs No. 2 and No. 3 operating are shown in Figure 6-2. During the time these results were collected, it was observed that the blades of the two operating turbines were rotating in synchronism, which is also evident from the results shown in Figure 6-2. The total signal variation obtained in Figure 6-1 is $\Delta \approx 15.7$ dB, which indicates that the amplitude

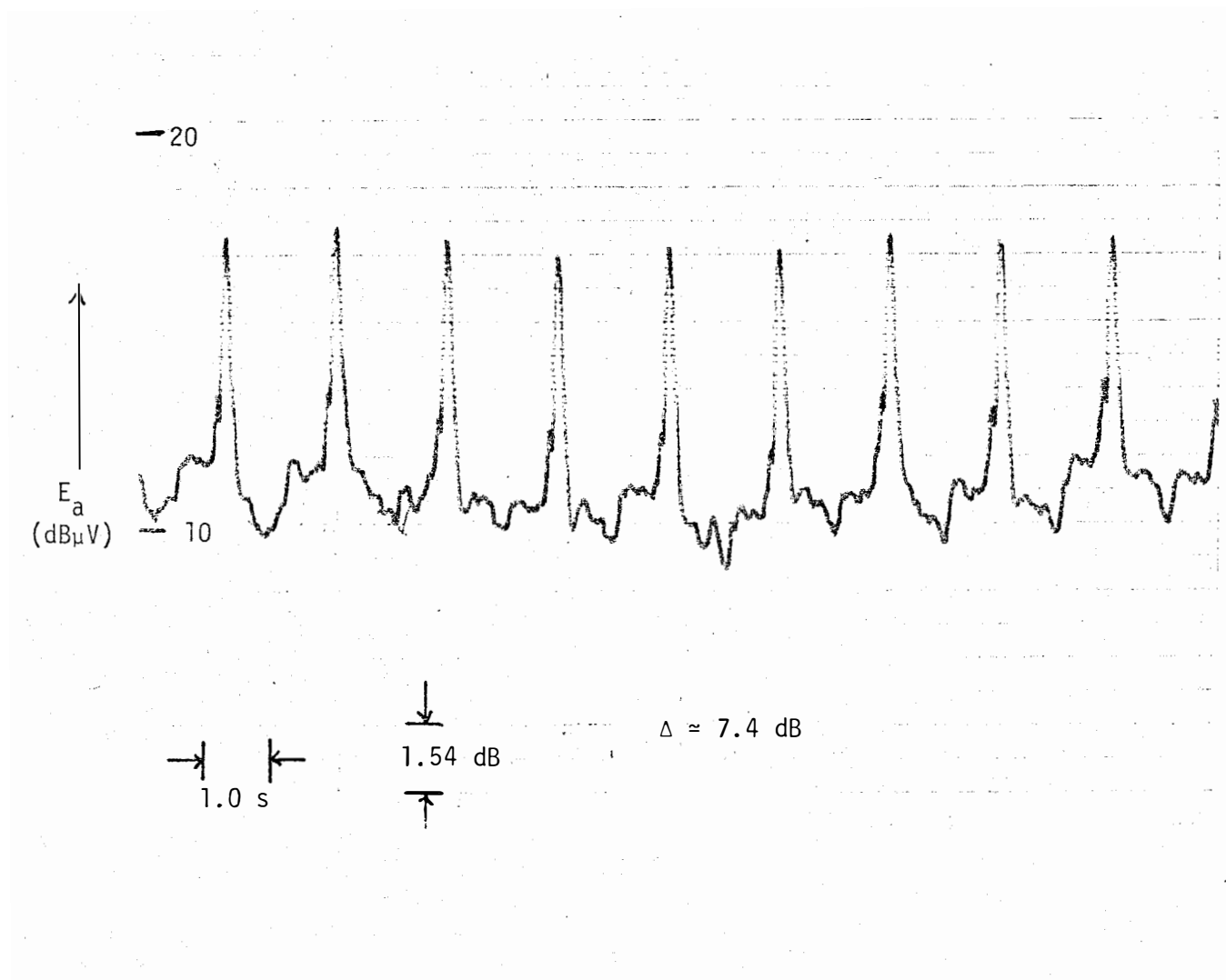


Figure 6-1. E_a (dB μ V) vs. Time on Channel 19, Obtained at Site A. WT No. 2 operating at 17.5 rpm. Receiving antenna directed toward the WT.

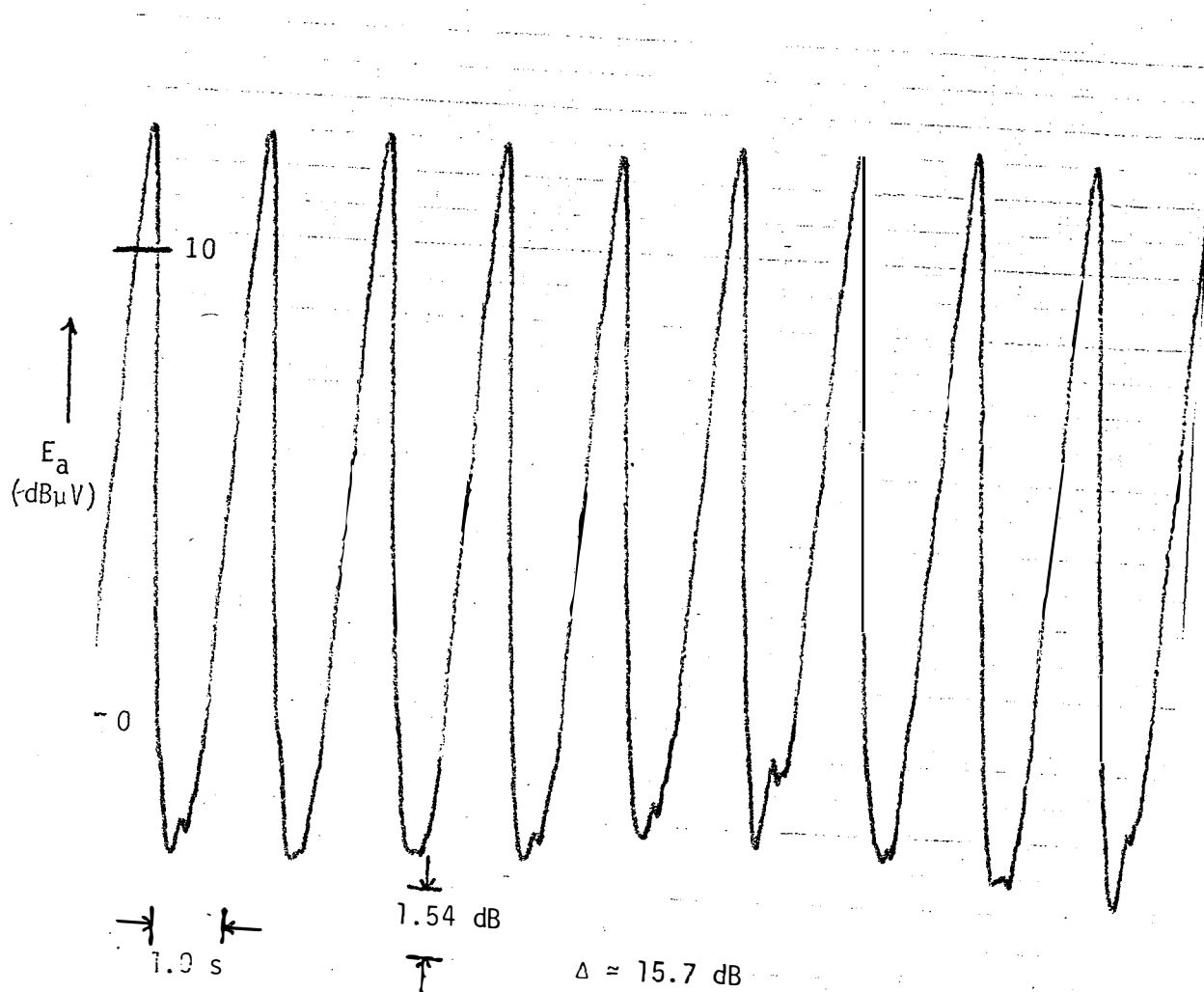


Figure 6-2. E_a ($\text{dB}\mu\text{V}$) vs. Time on Channel 19, Obtained at Site A. WTs No. 2 and No. 3 operating in synchronism at 17.5 rpm. Receiving antenna directed toward the WT array.

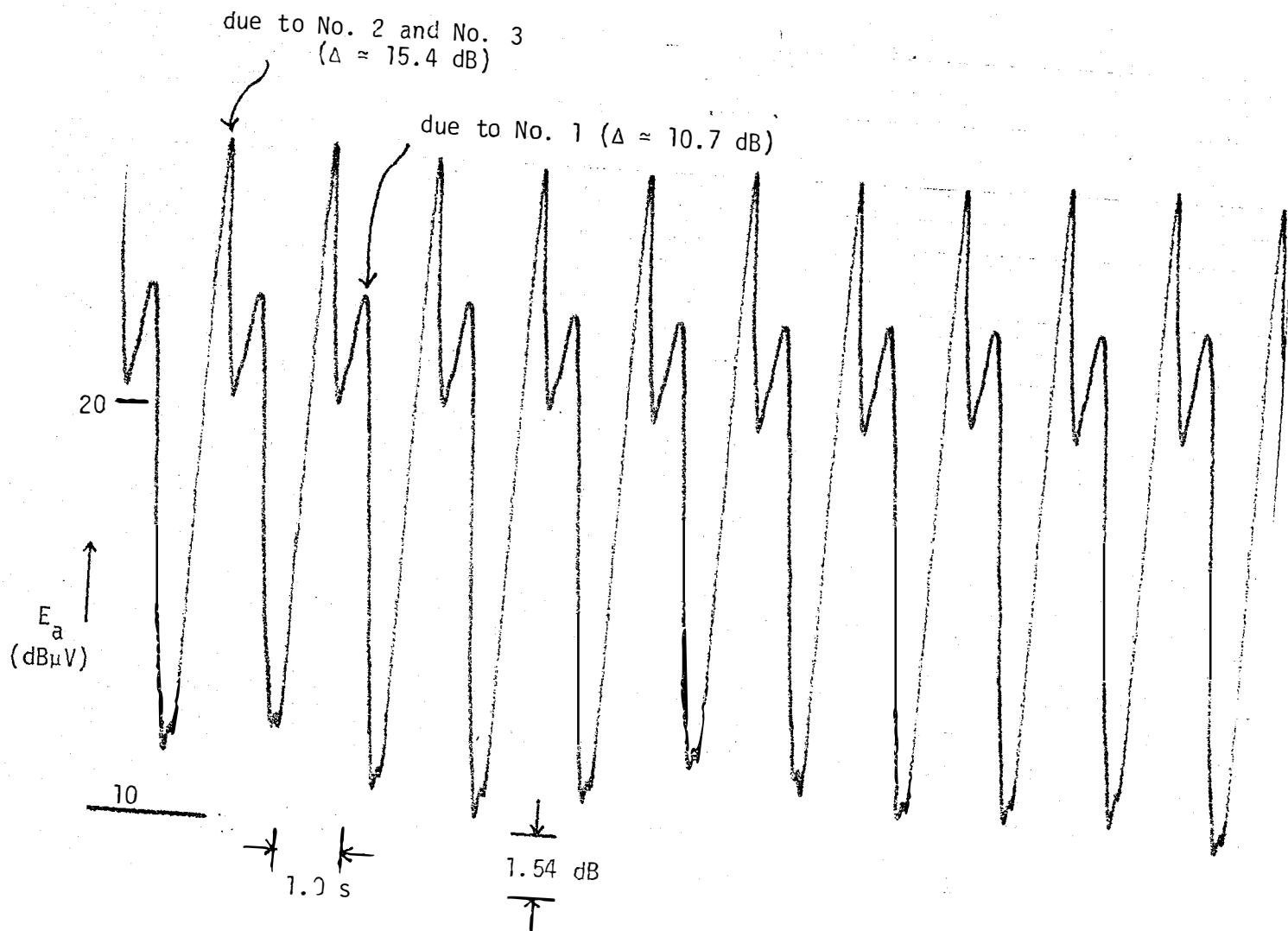


Figure 6-3. E_a (dB μ V) vs. Time on Channel 19, Obtained at Site A. WTs No. 1, No. 2, and No. 3 operating at 17.5 rpm, with No. 2 and No. 3 in synchronism. Receiving antenna directed toward the WT array.

of the received pulses was almost twice that of the pulses obtained with only one WT operating.

Figure 6-3 shows the results obtained with all three turbines operating, during which it was again observed that the blades of WTs No. 2 and No. 3 were rotating in synchronism. It is now argued that the larger amplitude pulses shown in Figure 6-3 were caused by the combined effects of scattering by the blades of WT No. 2 and No. 3, and the smaller amplitude pulses were caused by the WT No. 1 blade scattering.

Figure 6-4 shows similar data obtained on Channel 42 when the blades of the three turbines were rotating out of synchronism. Using a visual technique during the measurement, we were able to locate the individual pulses caused by the scattering by each of the machines, and these are identified in Figure 6-4. These results tend to be consistent with the geometry of the measurement at Site A. Referring to the map shown in Figure 2-2, we can see that WT Nos. 3, 2, and 1 are at increasing distances from Site A. In addition, from this site the WT No. 1 was partly shadowed by the WT No. 3. This may explain the decreasing amplitude of the interference pulses (Figure 6-4) caused by the WTs No. 3, 2, and 1, respectively.

The results presented in Figures 6-3 and 6-4 are unique in the sense that this was the only occasion where we were able to collect data with all three WTs operating. On that particular day, WT No. 1 operated about half the time, along with the other two machines. Later in the evening of that day, it was shut down and was not operated again during the rest of our test program.

6.2 SITE B

At this site, dynamic data were collected with WTs No. 3 and No. 2 operating singly and together. No appreciable TVI was observed on the UHF channels, and this was apparently because the WTs were located in the back lobe region of the antenna and oriented to receive maximum signals on the UHF channels originating from Pasco.

Figure 6-5 shows the results obtained where WT Nos. 2 and 3 are operating together and when the receiving antenna was oriented to receive signals on the VHF Channel 12 originating from Portland. The total variation in the received signals due to WT-interference, shown in Figure 6-5, is $\Delta \sim 2.46$ dB; some TVI effects were observed under these conditions.

6.3 SITE C

As shown in Table 4-3, the ambient signal levels on all of the available TV channels were extremely low at this site. As a result, the TV reception at Site C even under normal conditions was unacceptable, and no meaningful TVI measurements could be conducted with the receiving antenna pointed toward the desired TV transmitter. However, we obtained some dynamic results with the receiving antenna pointed toward the WT array so that the received scattered signals were appreciable and could be identified. These data were collected during the initial phase of our dynamic measurement program, and their purpose

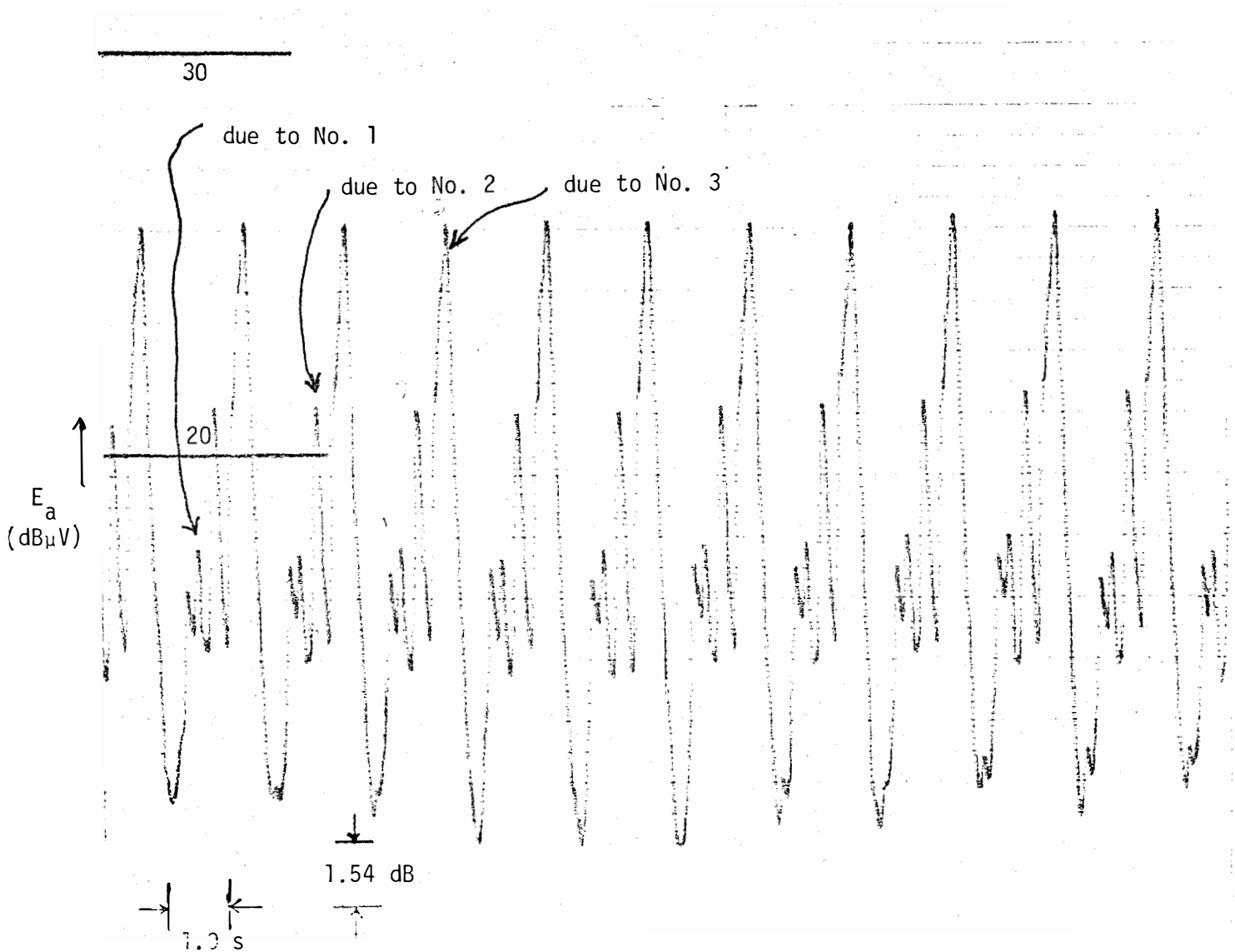


Figure 6-4. E_a ($\text{dB}\mu\text{V}$) vs. Time on Channel 42, Obtained at Site A. WTs No. 1 and No. 3 operating at 17.5 rpm, not in synchronism. Receiving antenna directed toward the WT array.

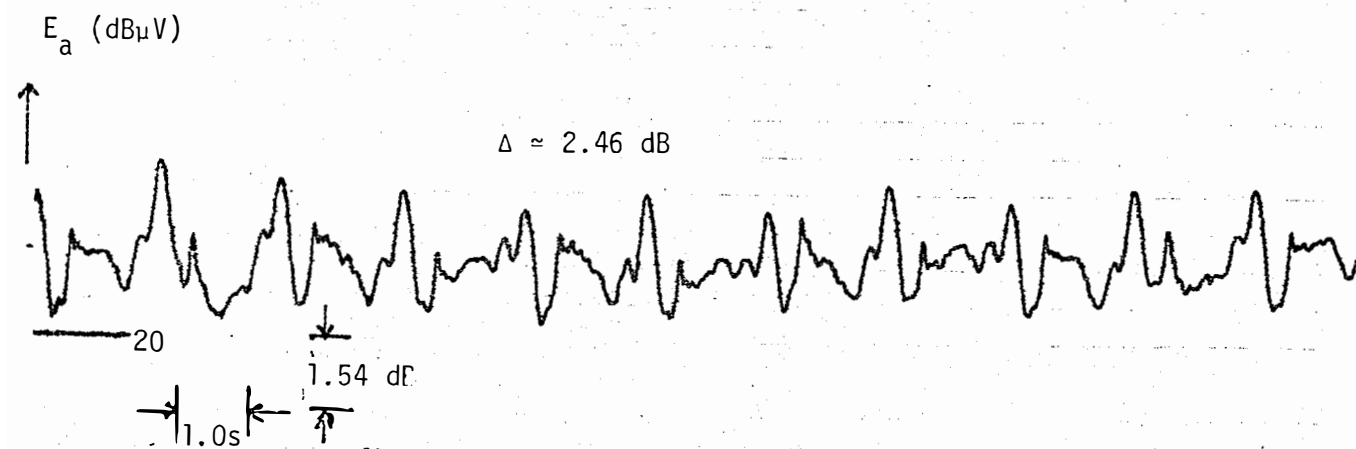


Figure 6-5. E_a (dB μ V) vs. Time on Channel 12, Obtained at Site B. WTs No. 2 and No. 3 operating at 17.5 rpm. Receiving antenna directed toward the transmitter.

was to study the general effects of the scattering by the WT. Received signal vs. time obtained on Channel 6 with WT No. 1 operating is shown in Figure 6-6, where the interference signals can barely be identified. Similar results obtained with WTs No. 1 and No. 3 operating are shown in Figure 6-7, where the pulsed signals caused by the scattering by the two machines may be clearly identified.

6.4 DISCUSSION

The quality of the TV reception on all of the available channels and in the vicinity of the WT array was poor to unacceptable, even under normal conditions; i.e., when the turbines were not operating and the receiving antenna beam was oriented in the direction of the desired TV station. Extremely weak ambient signals in the area made it very difficult to make complete TVI measurements at all of the test sites and on all the TV channels. With the antenna directed at the TV transmitter, although we did obtain interference pulses caused by the WT blade rotation, in many cases it was very difficult (if not impossible) to make any meaningful observations of the interference effects on the TV screen, because the signal strength was of the same order or below that of the noise level of the TV receiver. In one instance (at Site B, which was about one and one-half miles from the WT array site), we observed interference effects on the TV screen when the antenna was directed to receive signals from the Channel 12 transmitter at Portland.

The results obtained with the antenna beam directed toward the WT array are quite significant. It has been found that multiple WTs operating in synchronism tend to enhance the interference effects; in fact, our results indicate that two WTs operating in synchronism produced interference pulses whose amplitude was about twice that of the pulses caused by a single WT. When the machines do not operate in synchronism, they produce interference individually, and the interference pulses caused by each machine could be identified. Because the three WTs did not operate continually together, our results regarding the interference effects of the present WT array are not complete.

To fully understand the dynamic results, it is often necessary to have information regarding the yaw position and the pitch of the blades of the operating machines. During our measurement program, we estimated the yaw position of the WTs visually and found fair correlation with observed data. Since the teetering angle of the blades was variable and beyond control, it was impractical to try to determine the pitch of the blades. It is believed that the reduced amplitude interference pulses received at the test sites and on many channels were caused by the upward teetering of the blades (such blades scatter signals in directions above the horizon, thereby causing reduced amplitude scattered signals at the test sites which were below the elevation of the WT-blade centers).

Further study is recommended to evaluate the influence of the teetering angle of the blade and that of more than two WTs on the TVI effects produced.

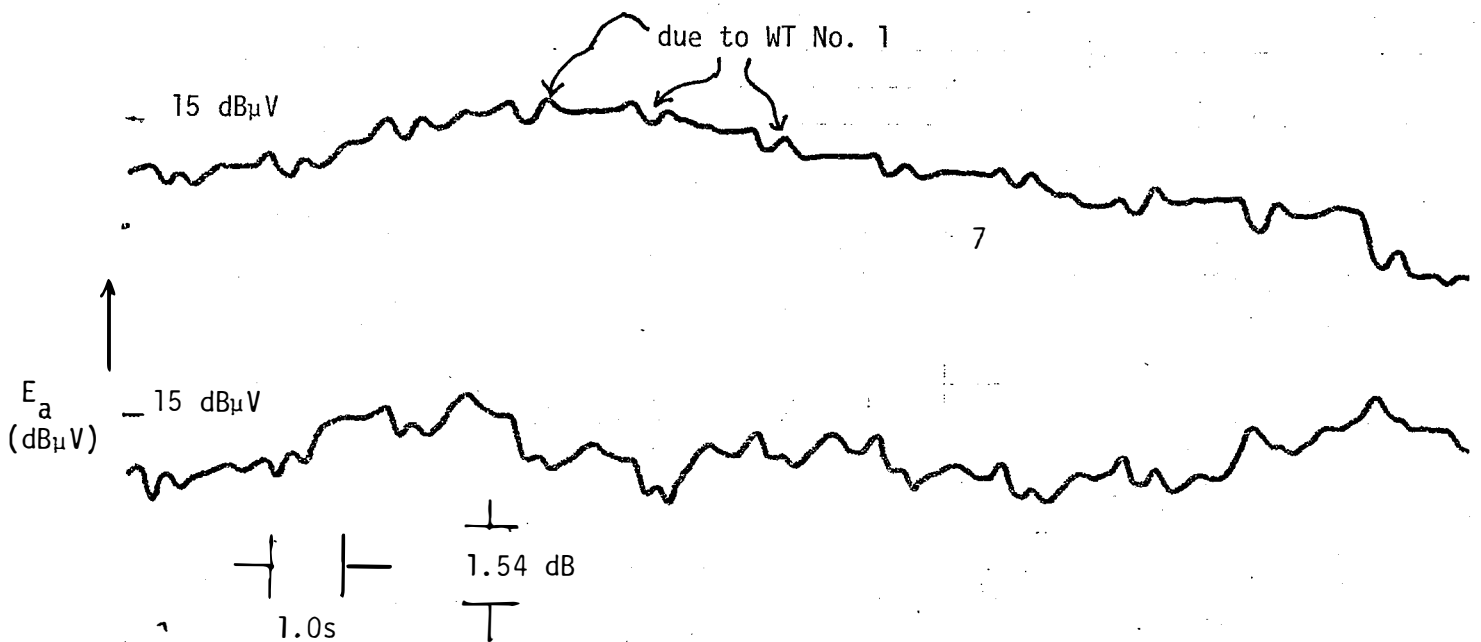


Figure 6-6. E_a (dB μ V) vs. Time on Channel 6, Obtained at Site C. WT No. 1 operating at 17.5 rpm. Receiving antenna directed at the WT.

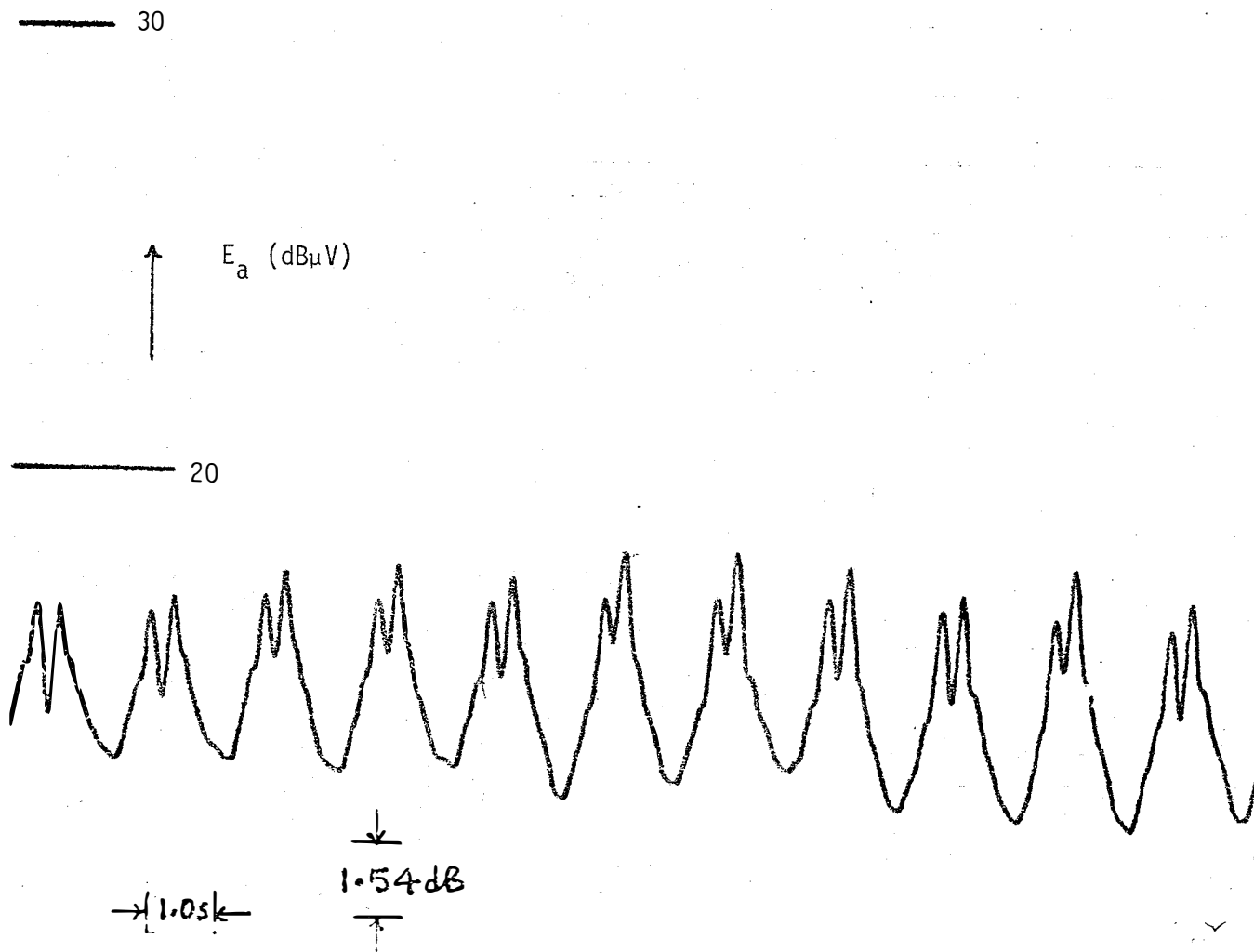


Figure 6-7. E_a ($\text{dB}\mu\text{V}$) vs. Time on Channel 6, Obtained at Site C. WTs No. 1 and No. 3 operating at 17.5, not in synchronism. Receiving antenna directed toward the WTs.

SECTION 7.0

CONCLUSIONS

The interference effects on TV reception caused by the MOD-2 WT array at Goodnoe Hills have been investigated by measuring the ambient field strengths, static (or blade) scattering, and TV interference at a number of locations in the vicinity of the WT array.

The most significant achievement has been the determination of the electromagnetic scattering parameters of the MOD-2 blade, which are required for estimating their interference effects on any electromagnetic system. The blade scattering parameters have been obtained from the results of static measurements by using an approximate theory based on the rectangular metal plate for the blade. Under zero pitch condition, the average scattering parameters determined from three independent static measurements are $A_e = 184 \text{ m}^2$; $L_1 = 85$, which should be compared with the value $A_e = 184 \text{ m}^2$; and $L_1 = 83 \text{ m}$, obtained from laboratory scale-model measurements. There is excellent agreement between the results obtained from the two types of measurements.

Because the ambient signals are extremely weak at all test locations, the quality of TV reception under normal conditions (i.e., receiving antenna beam oriented to receive maximum desired signal and the WTs not operating) was found to be poor to unacceptable there. Consequently, it was very difficult (if not impossible) to conduct meaningful dynamic or TVI measurements with the receiving antenna directed at the desired TV transmitter. Under this condition, we observed appreciable TVI effects on Channel 12 only at one location 1-1/2 miles from the WT array.

With the antenna beam directed at the WT array, some significant results were obtained with regard to the TVI effects produced by multiple WTs:

- Multiple WTs when operating in synchronism tend to enhance the TVI effects; in fact, our results indicate that two WTs operating in synchronism produce interference pulses whose amplitude was about twice that produced by a single WT.
- When the WTs do not operate in synchronism, they produce interference individually, and the interference pulses caused by each machine could be identified.

Our results regarding the interference effects of the present MOD-2 array are not complete. It is recommended that further dynamic measurements be conducted to

1. Obtain more detailed TVI effects produced by the WTs operating singly or in an array.
2. Evaluate the influence of the yaw position and the teetering angle of the blade.
3. Analyze the dynamic results using the approximate theory developed in Ref. 3.



SECTION 8.0**REFERENCES**

1. Linscott, B. S., J. T. Dennett, and L. H. Gordon, "The MOD-2 Wind Turbine Development Project," NASA Lewis Research Center Report, NASA TM-82681 (DOE/NASA/20305-5), July 1981.
2. Sengupta, D. L., T. B. A. Senior, and J. E. Ferris, "Television Interference Tests on Block Island, RI," University of Michigan Radiation Laboratory Report 014438-3-T, January 1980.
3. Sengupta, D. L., T. B. A. Senior, and J. E. Ferris, "Measurements of Interference to Television Reception Caused by the MOD-1 Wind Turbine at Boone, NC," University of Michigan Radiation Laboratory Report 018291-1-T, January 1981.
4. Senior, T. B. A., and D. L. Sengupta, "Large Wind Turbine Handbook: Television Interference Assessment," University of Michigan Radiation Laboratory Report 014438-4-T, April 1981.
5. Sengupta, D. L., and T. B. A. Senior, "Electromagnetic Interference by Wind Turbine Generators," University of Michigan Radiation Laboratory Report 014438-2-F, March 1978 (TID-28828).
6. Senior, T. B. A., D. L. Sengupta, and J. E. Ferris, "TV and FM Interference by Windmills," University of Michigan Radiation Laboratory Report 014438-1-F, February 1977.
7. Sengupta, D. L., and T. B. A. Senior, "Electromagnetic Interference to Television Reception Caused by Horizontal Axis Windmills," Proc. IEEE, Vol. 67, No. 8, pp. 1133-1142, August 1979.
8. Sengupta, D. L., and T. B. A. Senior, "Wind Turbine Generator Interference to Electromagnetic Systems," University of Michigan Radiation Laboratory Report 014438-3-F, August 1979.
9. Reference Data for Radio Engineers, Howard W. Sams & Co., Inc., Indianapolis, 1975, pp. 30-13, 30-15.
10. Senior, T. B. A., "Equivalent Scattering Area of the MOD-2 WT Blade," University of Michigan Radiation Laboratory Internal Memorandum No. 014438-555-M, 9 January 1980.
11. Stratton, J. A., Electromagnetic Theory, McGraw-Hill Book Co., Inc., New York, pp. 430-435, 1941.
12. Kerr, D. E., Propagation of Short Radio Waves, Boston Technical Publishers, Inc., Lexington, MA, pp. 34-41, 1964.



APPENDIX

THEORETICAL CONSIDERATIONS

Theoretical expressions used in Section 5.0 to determine the scattering parameters of the WT blade from static measurements are derived from the considerations of scattering of time harmonic plane electromagnetic waves by a rectangular metal plate.

A.1 SCATTERING BY A RECTANGULAR METAL PLATE

Let a rectangular metal plate of Length L_1 in the x-direction and width L_2 in the z-direction be located in the x-z plane of a rectangular coordinate system with origin 0, as shown in Figure A-1. The center of the plate is placed at 0, which is also the origin of a spherical coordinate system (r, θ, ϕ) . The plate is illuminated by a plane electromagnetic wave incident from the direction θ_i, ϕ_i with the electric vector polarized in the horizontal x-y plane such that the incident electric and magnetic vectors \vec{E}^i and \vec{H}^i are given by

$$\vec{E}^i = E_0 (\hat{x} \sin \phi_i - \hat{y} \cos \phi_i) \exp[ik(\sin \theta_i \cos \theta_i + y \sin \theta_i + \sin \theta_i + z \cos \theta_i)] , \quad (\text{A-1})$$

$$\vec{H}^i = H_0 (-\hat{x} \cos \theta_i \cos \phi_i - \hat{y} \cos \theta_i \sin \phi_i + \hat{z} \sin \theta_i) \times \exp[ik(\sin \theta_i \cos \phi_i + y \sin \theta_i \sin \phi_i + 2 \cos \theta_i)] , \quad (\text{A-2})$$

where

$E_0, H_0 = E_0/\eta_0$ are the amplitudes of the electric and magnetic vectors, respectively,

η_0 is the intrinsic impedance of the medium

$k = 2\pi/\lambda$ is the propagation constant in the medium, being the wavelength in the medium,

$\hat{x}, \hat{y}, \hat{z}$ are the unit vectors in the x, y, and z directions, respectively,

and a time dependence $\exp(i\omega t)$ is suppressed.

According to the physical optics approximation, the surface current density \vec{K} at an arbitrary point on the illuminated side of the plate is

$$\vec{K} = 2\hat{n} \times \vec{H}^i|_s , \quad (\text{A-3})$$

where $\vec{H}^i|_s$ is the incident magnetic field at the point on the plate, $\hat{n}(=\hat{y})$ is the unit normal on the illuminated side and $\vec{K} = 0$ on the shadowed side. In the present case, using Eqs. (A-2) and (A-3), we obtain the induced current density at a point r' on the plate as

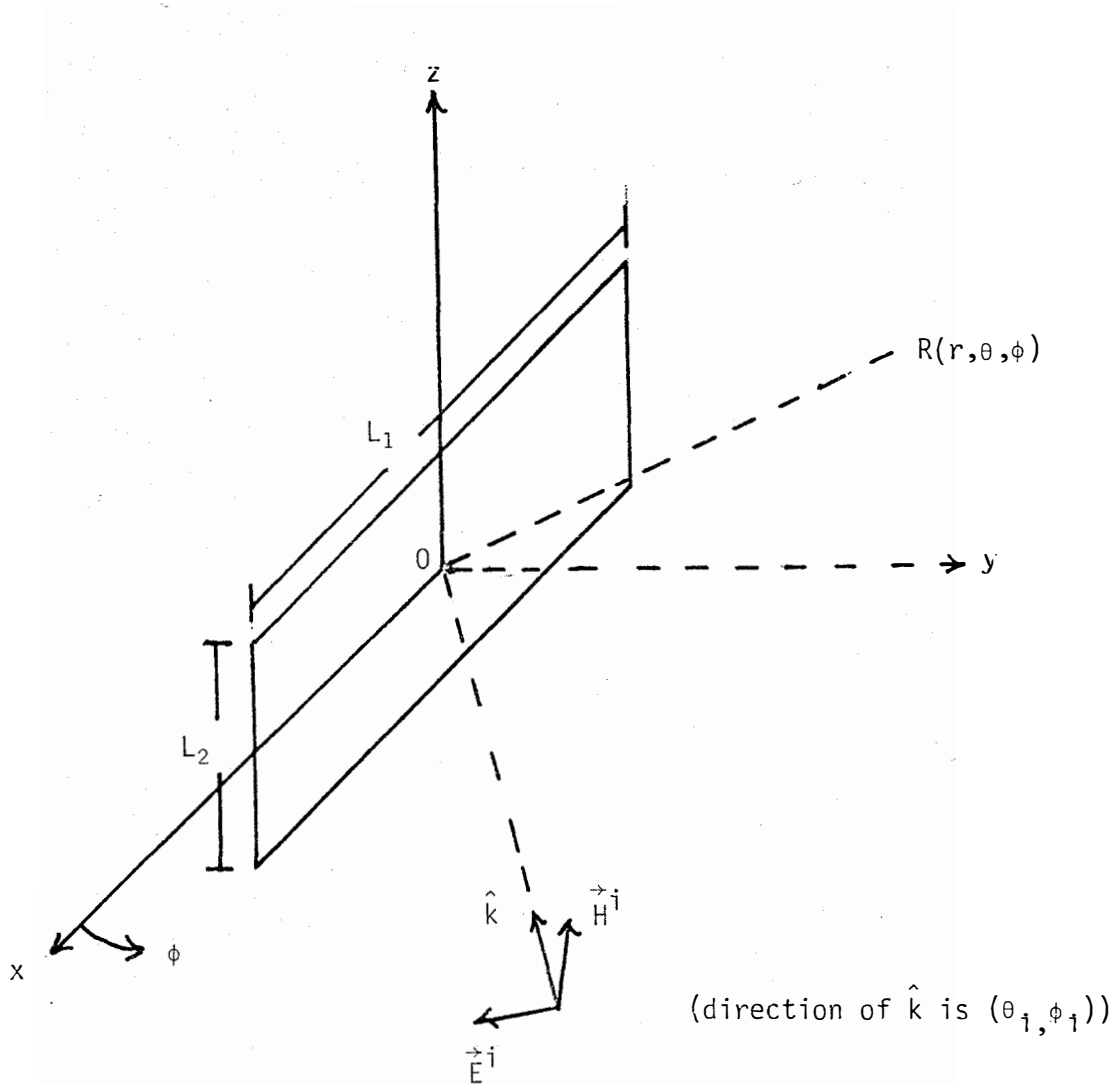


Figure A-1. Rectangular Metal Plate with the Incident Field Direction and the Receiver Location Shown

$$\vec{K}(\vec{r}') = 2H_0 [\hat{x} \sin \theta_i + \hat{z} \cos \theta_i \cos \phi_i] \exp[ik(x' \sin \theta_i \cos \phi_i + z' \cos \theta_i)] ,$$

$$\text{for } -\frac{L_1}{2} < x' < \frac{L_1}{2}$$

$$-\frac{L_2}{2} < z' < \frac{L_2}{2} = 0, \text{ otherwise}$$
(A-4)

where x' , z' refer to the coordinates of a point on the illuminated side of the plate.

The electric Hertz vector at a far field point $R(r, \theta, \phi)$ due to the current distribution $K(r')$ [11] is

$$\vec{\pi} = \frac{\eta_0}{4\pi k} \frac{\exp(-ikr)}{r} \int_S \vec{K}(\vec{r}') \exp(ik\hat{r} \cdot \vec{r}') dS' ,$$
(A-5)

where

$$\begin{aligned} \hat{r} &= \hat{x} \sin \theta \cos \phi + \hat{y} \sin \theta \sin \phi + \hat{z} \cos \theta \\ \vec{r}' &= \hat{x}x' + \hat{z}z' \\ dS' &= dx' dz' \end{aligned}$$
(A-6)

S = the surface area of the plate .

Hence, from Eqs. (A-4) through (A-6),

$$\begin{aligned} \vec{\pi} &= \frac{\eta_0 H_0 L_1 L_2}{2\pi k} \frac{\exp(-ikr)}{r} [\hat{x} \sin \theta_i + \hat{z} \cos \theta_i \cos \phi_i] \\ &\times \text{sinc} \left[\frac{L_1}{\lambda} (\sin \theta_i \cos \phi_i + \sin \theta \cos \phi) \right] \\ &\times \text{sinc} \left[\frac{L_2}{\lambda} (\cos \theta_i + \cos \theta) \right] , \end{aligned}$$
(A-7)

where

$$\text{sinc}[x] = \frac{\sin \pi x}{\pi x} .$$
(A-8)

Since the scattered electric field [11] is

$$\vec{E} = -k^2 [\hat{r} \times (\hat{r} \times \vec{\pi})] ,$$
(A-9)

and the transverse components of the scattered electric field at R are

$$E_\theta = -iE_0 \frac{L_1 L_2}{\lambda} \frac{\exp(-ikr)}{r} (\sin \theta_i \cos \theta \cos \phi - \cos \theta_i \sin \theta \cos \phi)$$

$$\begin{aligned} & \times \operatorname{sinc} \left[\frac{L_1}{\lambda} (\sin \theta_i \cos \phi_i + \sin \theta \cos \phi) \right] \\ & \times \operatorname{sinc} \left[\frac{L_2}{\lambda} (\cos \theta_i + \cos \theta) \right], \end{aligned} \quad (\text{A-10})$$

$$\begin{aligned} E_\theta &= iE_0 \frac{L_1 L_2}{\lambda} \frac{\exp(-ikr)}{r} (\sin \theta_i \sin \phi) \\ & \times \operatorname{sinc} \left[\frac{L_1}{\lambda} (\sin \theta_i \cos \phi_i + \sin \theta \cos \phi) \right] \\ & \times \operatorname{sinc} \left[\frac{L_2}{\lambda} (\cos \theta_i + \cos \theta) \right]. \end{aligned} \quad (\text{A-11})$$

To apply the above to the case of scattering by the WT blade, we assume $\theta_i = \pi/2$, $\theta = \pi/2 + \alpha$, and obtain the scattered fields as

$$\begin{aligned} E_\theta &= iE_0 \frac{L_1 L_2}{\lambda} \frac{\exp(-ikr)}{r} \sin \alpha \cos \phi \operatorname{sinc} \left[\frac{L_1}{\lambda} (\cos \phi_i + \cos \alpha \cos \phi) \right] \\ & \times \operatorname{sinc} \left[\frac{L_2}{\lambda} \sin \alpha \right], \end{aligned} \quad (\text{A-12})$$

$$\begin{aligned} E_\phi &= iE_0 \frac{L_1 L_2}{\lambda} \frac{\exp(-ikr)}{r} \sin \phi \operatorname{sinc} \left[\frac{L_1}{\lambda} (\cos \phi_i + \cos \alpha \cos \phi) \right] \\ & \times \operatorname{sinc} \left[\frac{L_2}{\lambda} \sin \alpha \right]. \end{aligned} \quad (\text{A-13})$$

For the purpose of analyzing the results of static measurements, it is of interest to obtain the scattered fields under conditions when the plate is slowly rotating in the horizontal plane, and the incident and scattered field directions are constant. It is now assumed that the bistatic angle, $2\phi_0 = \phi_i - \phi$, between the scattered and incident direction is constant, and that the plate rotation angle β is measured anticlockwise from the meridian plane bisecting the bistatic angle (see Figure 5-4). Under these conditions, it can be shown that Eqs. (A-12) to (A-13) reduce to

$$\begin{aligned} E_\theta &= -iE_0 \frac{A_e}{\lambda} \frac{\exp(-ikr)}{r} \sin \alpha \sin(\phi_0 - \beta) \\ & \times \operatorname{sinc} \left[\frac{L_1}{\lambda} \{ \sin(\phi_0 + \beta) - \cos \alpha \sin(\phi_0 - \beta) \} \right] \\ & \times \operatorname{sinc} \left[\frac{L_2}{\lambda} \sin \alpha \right], \end{aligned} \quad (\text{A-14})$$

$$\begin{aligned} E_\phi &= iE_0 \frac{A_e}{\lambda} \frac{\exp(-ikr)}{r} \cos(\phi_0 - \beta) \operatorname{sinc} \left[\frac{L_1}{\lambda} \{ \sin(\phi_0 + \beta) - \cos \alpha \sin(\phi_0 - \beta) \} \right] \\ & \times \operatorname{sinc} \left[\frac{L_2}{\lambda} \sin \alpha \right], \end{aligned} \quad (\text{A-15})$$

where

$$A_e = L_1 L_2 \cdot \quad (\text{A-16})$$

It can be seen from Eqs. (A-14) and (A-15) that

$$\left| \frac{E_\theta}{E_\phi} \right| = \left| \sin \alpha \tan(\phi_0 - \beta) \right| \cdot \quad (\text{A-17})$$

Usually, $\alpha \approx 0$ and $\phi_0 \ll \pi/4$. Thus, (A-17) indicates that near the specular position of the plate (i.e., $\beta \approx 0$),

$$|E_\theta| \ll |E_\phi| ,$$

which means that the horizontal component (E_ϕ) of the scattered field is predominant at R, and which is of interest in the present case.

A.2 RECEIVED FIELD DURING STATIC MEASUREMENTS

The rectangular plate in Figure A-1 is now identified as the WT blade with O coinciding with the phase center B of the blade. Figures 5-4 and 5-5 are horizontal and vertical plane views, respectively, of the geometry where R and B are the (phase) centers of the receiving antenna and the plate, and T is the transmitter. Under free space conditions, the scattered field at R is given by Eq. (A-15). On the assumption that the entire system is located above a homogeneous flat earth, the amplitude of the scattered field at R as a function of β [3,7] is

$$E^S(R) = F E_a(B) \frac{A_e}{\lambda} \cos(\phi_0 - \beta) \left| \left[\text{sinc} \left[\frac{L_1}{\lambda} \{ \sin(\phi_0 + \beta) - \cos \alpha \sin(\phi_0 - \beta) \} \right] \cdot \left| \text{sinc} \left[\frac{L_2}{\lambda} \sin \alpha \right] \right| \right] \right| , \quad (\text{A-18})$$

where

$$F = \left\{ (1 - |P|)^2 + 4|\Gamma|^2 \sin^2 \left[\frac{2\pi h_a h_t}{\lambda r} \right] \right\}^{1/2} ,$$

$$r = \{D^2 + (h_t - h_a)^2\}^{1/2} ,$$

$$\alpha = \tan^{-1} \frac{h_t - h_a}{D} , \quad (\text{A-19})$$

$E_a(B)$ is the ambient (incident) field strength at B, $|\Gamma|$ is the amplitude of the reflection coefficient for grazing incidence on the ground, and other parameters are indicated in Figures 5-4 and 5-5. The quantity F includes the effects of reflection from the ground at near grazing angles [12].

The scattered field at R is a maximum when $\beta = 0$, and as a function of the blade rotation, the amplitude modulation index m of the signal received with a directional antenna having its main beam pointed at B [7] is

$$m = \frac{E^S(R) \big|_{\beta=0}}{E_{av}} , \quad (\text{A-20})$$

where E_{av} is the received ambient field strength at R.

In the present case, the terrain conditions are such that $|\Gamma| = 0$. Under this condition from Eqs. (A-18) and (A-20), the equivalent scattering area A_e and the length L_1 of the blade are

$$A_e = \frac{\pi \lambda r}{\frac{E_a(B)}{E_{av}} \cos \phi_0 \text{sinc}_1 \text{sinc}_2} \quad (\text{A-21})$$

$$L = \frac{\lambda}{(1 - \cos \alpha) \sin \phi_0 \cos \beta_0 + (1 + \cos \alpha) \cos \phi_0 \sin \beta_0} \quad (\text{A-22})$$

$$\approx \frac{0.5 \lambda}{\cos \phi_0 \sin \beta_0}, \text{ for } \alpha \approx 0,$$

where

$$\text{sinc}_1 = \frac{\sin \pi x_1}{\pi x_1}, \text{ sinc}_2 = \frac{\sin \pi x_2}{\pi x_2}, \quad (\text{A-23})$$

$$x_1 = \frac{L_1}{\lambda} \{ (1 - \cos \alpha) \sin \alpha \}, \quad (\text{A-24})$$

$$x_2 = \frac{L_2}{\lambda} \sin \alpha. \quad (\text{A-25})$$

$2\beta_0$ = the angle between the nulls of the main scattering lobe of the received field.

Equations (A-21) through (A-25) are the same as Eqs. (5-1) through (5-5) in Section 5.4.

Document Control Page	1. SERI Report No. STR-211-2086	2. NTIS Accession No.	3. Recipient's Accession No.
4. Title and Subtitle Television Interference Measurements Near the MOD-2 WT Array at Goodnac Hills, Washington		5. Publication Date November 1983	6.
7. Author(s) D. L. Sengupta, T. B. A. Senior, J. E. Ferris, Niel Kelley, Bob Noun		8. Performing Organization Rept. No.	
9. Performing Organization Name and Address Radiation Laboratory Department of Electrical and Computer Engineering The University of Michigan Ann Arbor, Michigan 48109		10. Project/Task/Work Unit No. 1066.70	11. Contract (C) or Grant (G) No. (C) DE-AC02-76ET20234 (G)
		12. Sponsoring Organization Name and Address Solar Energy Research Institute 1617 Cole Boulevard Golden, Colorado 80401	
13. Type of Report & Period Covered Technical Report		14.	
15. Supplementary Notes Technical Monitor: Neil Kelley			
16. Abstract (Limit: 200 words) Electromagnetic interference to television reception caused by the MOD-2 wind turbine (WT) array at Goodnoe Hills, Wash., was studied by means of detailed measurements at a number of test sites in the vicinity of the WT array. The commercial television signals available in the area were used as the radio frequency sources during the measurements. The dynamic measurements indicated that varying amounts of TVI were produced at all sites and on some or all of the available TV channels; with the directional antenna in use, most of the backward region interference produced video distortion that was judged to be acceptable; at one test location about 1-1/2 miles from the WT array site, forward region interference was observed; when the blades of the WTs rotate in synchronism, they tend to increase the amplitude of the interference pulses, thereby producing more TVI effects; and when the blades do not rotate in synchronism, each WT produces interference effects individually.			
17. Document Analysis a. Descriptors Antennas ; Interference ; Television ; Turbine Blades ; Wind Turbines b. Identifiers/Open-Ended Terms c. UC Categories 60			
18. Availability Statement National Technical Information Service U.S. Department of Commerce 5285 Port Royal Road Springfield, Virginia 22161		19. No. of Pages 64	20. Price A04